Phil. Trans. R. Soc. Lond. A **327**, 337–363 (1988) [337]
Printed in Great Britain

Quaternary and active faulting observed on the 1985 Academia Sinica–Royal Society Geotraverse of Tibet

By William S. F. Kidd[1] and Peter Molnar[2]

[1] *Department of Geological Sciences, State University of New York, Albany, New York* 12222, *U.S.A.*
[2] *Department of Earth, Atmospheric, and Planetary Sciences, Massachusetts Institute of Technology, Cambridge, Massachusetts* 02139, *U.S.A.*

[Plates 1–13]

Active and recent faulting along the main north–south road in Tibet is dominated by normal faulting occurring on northerly-trending planes and by strike-slip faulting, both of which reflect an east–west extension of the plateau. Normal faulting is prevalent in the southern half of the plateau, but we saw no evidence for any major graben in the northern half. Strike-slip faulting on roughly easterly-trending structures is more prevalent in the northern half, but conjugate faulting, with right-lateral slip on northwesterly-trending planes and left-lateral slip on north-easterly-trending planes, is common in the southern half. In two areas, we also observed components of thrust faulting, apparently in association with young strike-slip faulting.

Our most important results are bounds on the rates of slip on the two main strands of the Kunlun strike-slip fault system, which trends east–west through the Kunlun range. Ground moraine containing boulders of pyroxenite is separated by 30 km from the nearest outcrop of such rock, implying that amount of displacement in the last 1.5 to 3 Ma. Therefore the average rate of slip during the Quaternary period has been between 10 and 20 mm/a, with a likely value of 13 mm/a. Abundant fresh tension cracks and mole tracks imply continued slip on the main strand, the Xidatan–Tuosuohu–Maqu fault, and the likely occurrence of a major earthquake in the last few hundred years. Consistent offsets of gullies and dry stream channels of about 10 m may reflect slip of that amount during such an earthquake, and possible multiple offsets at one site suggest that slip may occur by large displacements of 10 m during infrequent great earthquakes. Along the other strand, the Kunlun Pass fault, offsets of roughly 50 to 150 m of, apparently, post-glacial valleys and of one glacier and its terminal moraine suggest a Holocene rate of slip between 5 and 20 mm/a, and most likely about 10 mm/a, on this fault. These rapid rates of displacement imply that Tibet is being extruded rapidly eastward, at a rate comparable to the rate at which India is penetrating into Eurasia, and therefore that, at present, a substantial fraction of this penetration is being absorbed by the eastward extrusion of Tibet.

Introduction

The study of Quaternary and active faulting of Tibet essentially began in the early 1970s with the study of Landsat imagery, or perhaps a decade earlier with the installation of the World-Wide Standardized Seismograph Network (WWSSN). Most early explorers of Tibet had little or no geologic training and made few useful geologic observations. An exception was Littledale

(1896), whose accurate mapping of young volcanoes was particularly useful to us, among others, in our first studies of Tibet (Burke *et al.* 1974; Kidd 1975; Molnar & Tapponnier 1978; Sengör & Kidd 1979). Nevertheless, even those who took care to gather geologic samples, such as Sven Hedin (see Hennig 1915), were less concerned with geologic structures, particularly with recent ones, than with collecting representative examples of particular rock types. Erik Norin, perhaps the first geologist to carry out serious geologic mapping within Tibet, described folding and thrust faulting of Tertiary sedimentary rock on the northern margin of western Tibet (Norin 1946), but even he wrote little about Quaternary or active deformation on the plateau itself. Thus when the Landsat imagery became available, a wealth of information was suddenly available to be gleaned.

Studies both of the Landsat imagery and of the larger earthquakes ($M \geqslant 5.5$) indicate that the most recent deformation is by normal and strike-slip faulting (Armijo *et al.* 1986, in press; Molnar & Chen 1983; Molnar & Tapponnier 1975, 1978; Ni & York 1978; Rothery & Drury 1984; Tapponnier & Molnar 1977; Tapponnier *et al.* 1981*a*, 1981*b*). Several north–south trending grabens are clear on the satellite imagery of southern Tibet (Armijo *et al.* 1986; Tapponnier *et al.* 1981*b*), and nearly all fault plane solutions of earthquakes in southern Tibet indicate large components of normal faulting (Molnar & Chen 1983; Molnar & Tapponnier 1978; Ni & York 1978). Some grabens in southern Tibet are linked by strike-slip faults (figure 1) (Armijo *et al.* 1986), and several metres of right-lateral slip on a northwest-trending fault can be associated with the largest earthquake (18 November 1951; $M = 8$) to have occurred within the Tibetan plateau in this century (Armijo *et al.* in press). Both fault plane solutions and structures visible on the Landsat imagery indicate a greater significance of strike-slip faulting in central and northern than southern Tibet (Armijo *et al.* in press; Molnar & Chen 1983; Molnar & Tapponnier 1978; Rothery & Drury 1984). Short strike-slip faults seem to link normal faults so as to form a mosaic of blocks that move with respect to one another and to yield an average east–west extensional regional strain (Rothery & Drury 1984). Farther north, near the edge of the plateau, left-lateral slip on the Altyn Tagh and Kunlun fault systems (figure 1) accommodates an eastward displacement of Tibet with respect to the areas to the north, the Tarim and Qaidam basins and the Nan Shan (Molnar & Tapponnier 1975; Tapponnier & Molnar 1977).

The strike-slip faulting within Tibet, on northwest- and northeast-trending planes, reflects some active north–south shortening of the plateau (Rothery & Drury 1984), perhaps as rapidly as half of the rate at which it extends in an east–west direction (Molnar & Chen 1983). Although there is abundant evidence for thrust-faulting and folding of Tertiary rock on the margins of the plateau (figure 1), i.e. in the Himalaya, in the Altyn Tagh (Molnar *et al.* 1987*a*, 1987*b*), or on the northeast edge of the plateau (Burchfiel *et al.* in press), there is little evidence for active or recent north–south crustal shortening by thrust or reverse faulting or by folding *within* the high plateau. No reliable fault plane solution of an earthquake within the high plateau shows a significant reverse or thrust component (Molnar & Chen 1983); and, in general, structures suggestive of folding or reverse faulting that can be recognized from the Landsat imagery are cut by recent normal or strike-slip faults (Armijo *et al.* 1986; Molnar & Tapponnier 1978; Ni & York 1978; Rothery & Drury 1984). Thus the prevalence of normal and strike-slip faulting requires a change in the style of deformation from that which built the plateau; the abundant evidence for Tertiary north–south crustal shortening (Chang *et al.* 1986; Dewey, Shackleton, Chang & Sun, this volume) contrasts markedly with the present style of deformation.

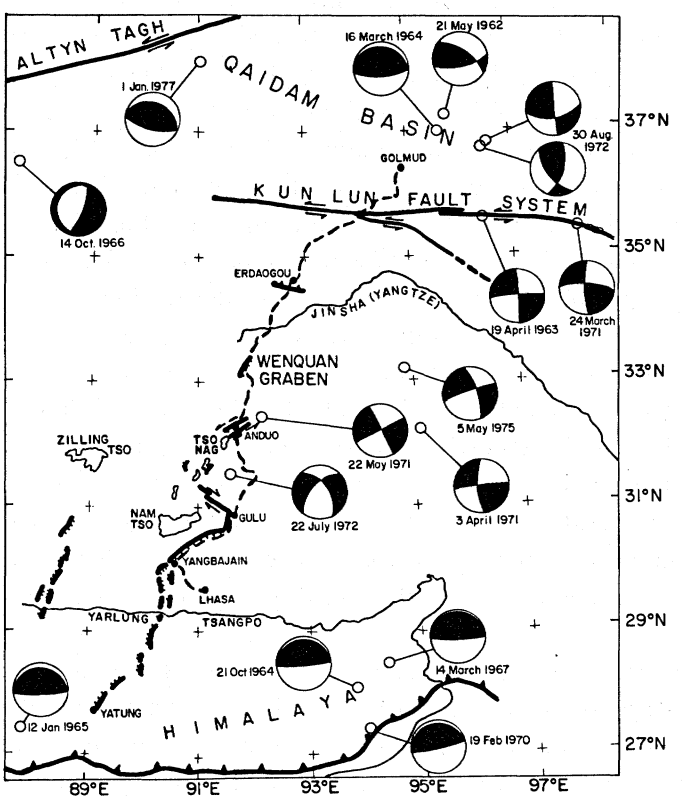

FIGURE 1. Map of the region of Tibet traversed, showing the main road, major towns, rivers, and faults, and lower hemisphere projections of fault plane solutions of earthquakes. The numerous examples of active normal faulting in southern Tibet, shown by dark lines with teeth on the downthrown side, were taken from Armijo *et al.* (1986). Note how the Kunlun Pass fault curves southward to the east, and how the Xidatan–Tuosuohu–Maqu fault continues west for several hundred km. For fault plane solutions, taken from Molnar & Chen (1983), Molnar & Tapponnier (1978), Molnar *et al.* (1977), and Tapponnier & Molnar (1977), the darkened quadrants contain compressional first motions, and therefore the T-axes.

The studies of the Landsat imagery and of seismicity have provided a general, qualitative description of the active and recent deformation of Tibet, but what clearly cannot be learned from them are tight constraints on the amounts, the timing, and the rates of these processes. One of the important questions to be answered surely is: When did the change from folding and thrust faulting to normal faulting and east–west extension occur? It is likely that this change took place at different times at different places. The folding of Pliocene sedimentary rock in the Lunpola basin [east of Zilling Tso (figure 1)] (Burke & Lucas in press; Lee 1984), and the overthrusting of (possibly late) Neogene sedimentary rock 15 km south of Erdaogou (figure 1) (Chang *et al.* 1986; Dewey, Shackleton, Chang & Sun, this volume) imply that crustal shortening must have occurred, at least in some parts of Tibet, in late Tertiary time and perhaps during the Quaternary period. Correspondingly, from the distribution and the disruption of moraines presumed to be of Quaternary age, Armijo *et al.* (1986) inferred that the normal faulting in southern Tibet did not begin until Quaternary time. Unfortunately, however, as discussed by Smith & Xu (this volume), the ages of Tertiary and Quaternary rocks are not well constrained, so that precise dating of late Cenozoic folding and faulting is difficult. Nevertheless, taken together the evidence suggests that the initiation of the present style of deformation began relatively recently in geologic time.

An important goal of many geologists studying the late Cenozoic tectonics of Asia is the determination of how much Tibet has been extruded eastward out of the way of India's path toward the rest of Asia (e.g. Armijo *et al.* in press; Molnar & Deng 1984; Molnar & Tapponnier 1975; Tapponnier *et al.* 1982, 1986). Accordingly, we seek answers to: How much displacement has occurred on the strike-slip and normal faults? How far has Tibet slid eastward with respect to the Tarim Basin, and how much extension has occurred within Tibet? Related to these questions is: What is the average rate of slip on individual faults?

In the first attempt to address any of these questions with geologic data, Armijo *et al.* (1986) studied two of seven prominent graben systems in southern Tibet, and from their inferred rate of extension in one, the Yatung–Yangbajain–Gulu 'rift' (figure 1), they made a seven-fold extrapolation to estimate an overall rate of extension across the plateau of 10 ± 5 mm/a. Armijo *et al.* (in press) estimated rates of slip of 10 to 20 mm/a on short, WNW-trending right-lateral strike-slip faults that lie north of the rifts. Presuming these strike-slip faults to be linked to a major right-lateral shear zone in south central Tibet, they inferred a rapid eastward extrusion of Tibet at a rate of tens of mm/a. Despite the care with which their studies were made, however, much more field work will be needed before their extrapolated and inferred rates can be tested and before most of these questions can be given quantitatively meaningful answers.

It should be noted that the study of active and recent deformation was not one of the major objectives of the Academia Sinica/Royal Society Geotraverse, for there was rarely time to carry out the detailed investigations needed to make quantitative measurements of amounts, ages, or rates of deformation. Moreover, we were both familiar with the preliminary work on the active tectonics of southern Tibet (Tapponnier *et al.* 1981*a*, 1981*b*) and aware that Armijo *et al.* (1986, in press) had already carried out a more detailed study than we would be able to make in the portion of southern Tibet that we traversed. Thus, our focus was on the area north of where Armijo, Tapponnier and their colleagues had worked, and specifically on the Kunlun strike-slip fault system (figure 1), by far the most significant fault system that we crossed. Consequently we addressed, in essence, only one of the basic questions noted above; we sought constraints on the rates of slip on the two main segments of the Kunlun strike-slip fault system.

Although the bulk of this chapter addresses the evidence for Quaternary to recent activity on the Kunlun fault system, we report a few observations made in areas not studied by Armijo *et al.* (1986, in press) or Tapponnier *et al.* (1981*a*, 1981*b*). Before describing these, however, it is worth noting that in our brief reconnaissance of the Yangbajain–Gulu areas (figure 1), where we saw many of the spectacular examples of recent faulting described by Armijo *et al.* (1986), we saw no evidence of any process inconsistent with those inferred to have operated by Armijo *et al.* (1986, in press), from their more extensive observations.

Active faulting in the central part of the traverse

Armijo *et al.* (1986) described in detail a graben system that extends north from south of the Yarlung Zangbo through Yangbajain and Gulu and possibly northeast as far as the lake Tso Nag (figure 1). Tso Nag seems to lie in a northerly-trending graben or half-graben; a metric camera satellite photograph shows a clear scarp on its east side (A in figure 2). Northeast of Tso Nag, northeast-trending linear escarpments are also clear on the satellite photo (B and C

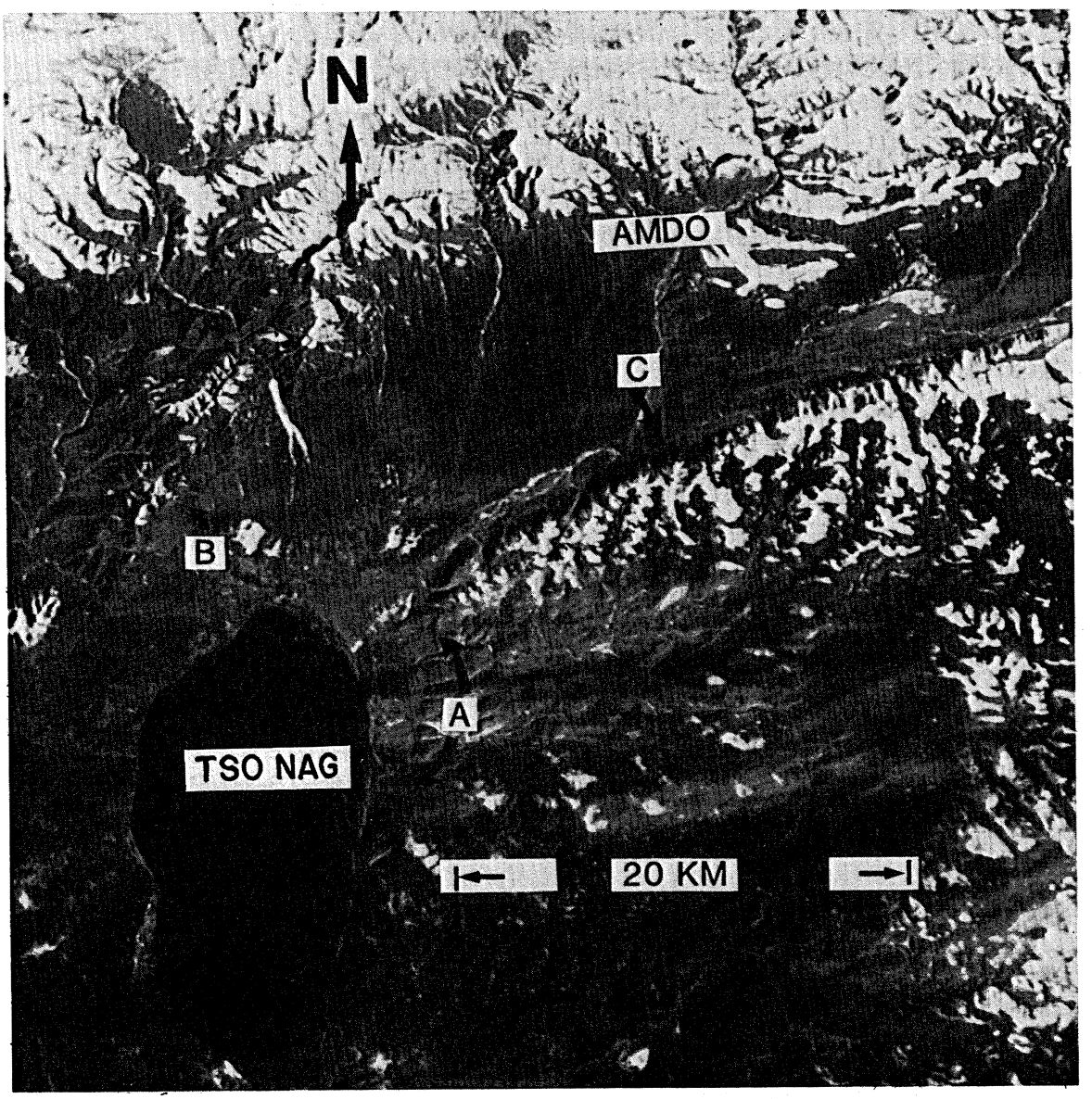

FIGURE 2. Portion of a shuttle metric camera photograph showing the area near Amdo and the lake Tso Nag (figure 1). Note the clear scarp on the east side of Tso Nag (A), which we presume to mark an active or recently active normal fault. To the northeast, the valley containing the town of Amdo is bounded by linear scarps, along which we think there is a large strike-slip component. At C, recent sand and gravel is disrupted (figure 3). At B, there is a component of thrust or reverse faulting, but the linearity of the scarp suggests that there is a significant strike-slip component.

(*Facing p.* 340)

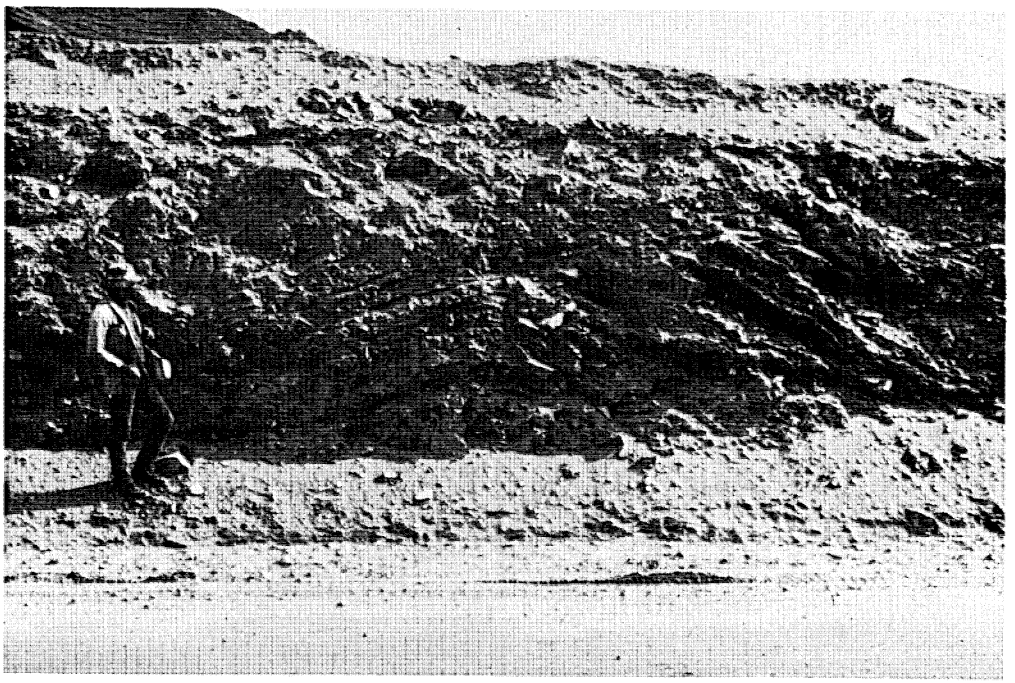

FIGURE 3. Photograph, taken at C in figure 2, showing folded and faulted layers of sand and gravel along a zone where oblique normal and left-lateral strike-slip faulting seems to have occurred. The view is to the south.

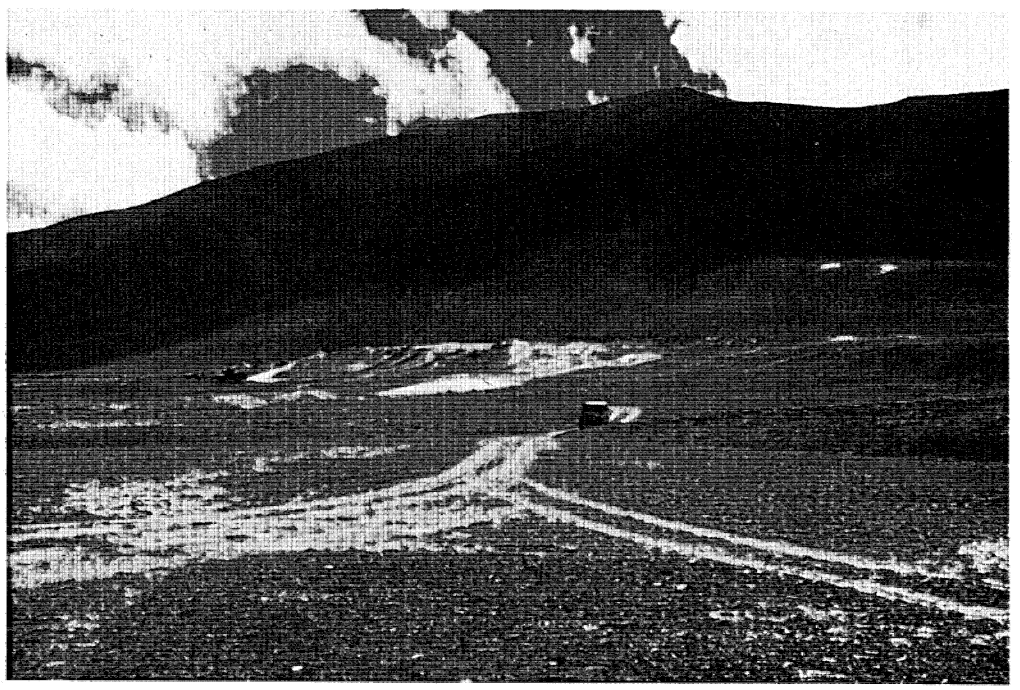

FIGURE 4. Photograph of young scarp near hot springs on the west side of a graben (or half-graben) near Wenquan (figure 1). View is to the west-southwest.

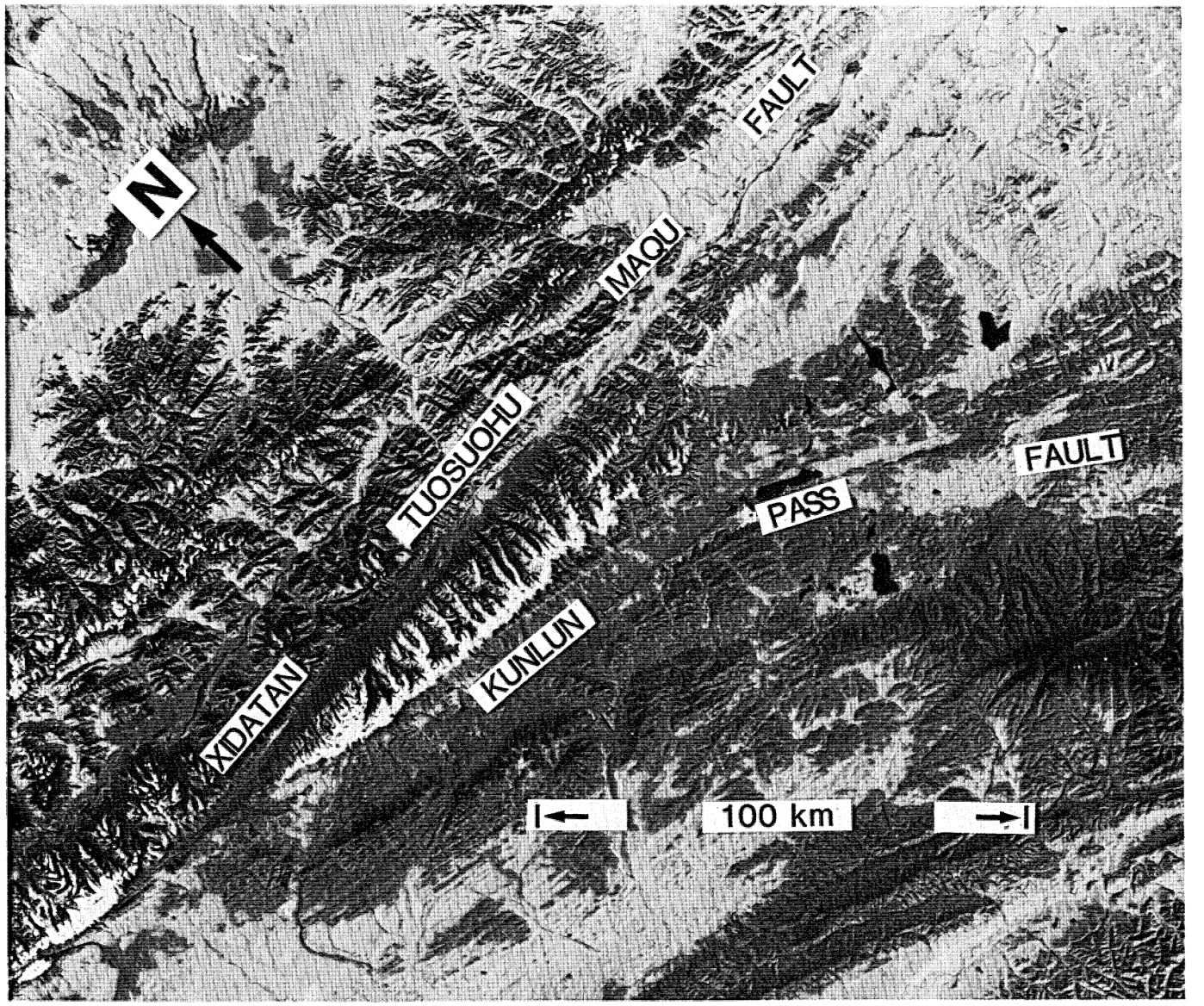

FIGURE 5. Large format camera photograph of the area including the Xidatan, Burhan Budai, and Kunlun Pass region. The Burhan Budai is the easterly-trending snow-capped range in the west-central part of the image between the Xidatan–Tuosuohu–Maqu and Kunlun Pass faults. The Xidatan–Tuosuohu–Maqu fault passes north of the Burhan Budai through the easterly-trending valleys, the Xidatan (figures 7 and 8) and Dongdatan (figures 23 and 31), and continues into a large pull-apart structure (figure 31). South of the Burhan Budai the Kunlun Pass fault is visible at the break in slope at the foot of the range (figure 14). Toward the west the Kunlun Pass fault approaches the Xidatan–Tuosuohu–Maqu fault but does not appear to intersect it (see figure 8).

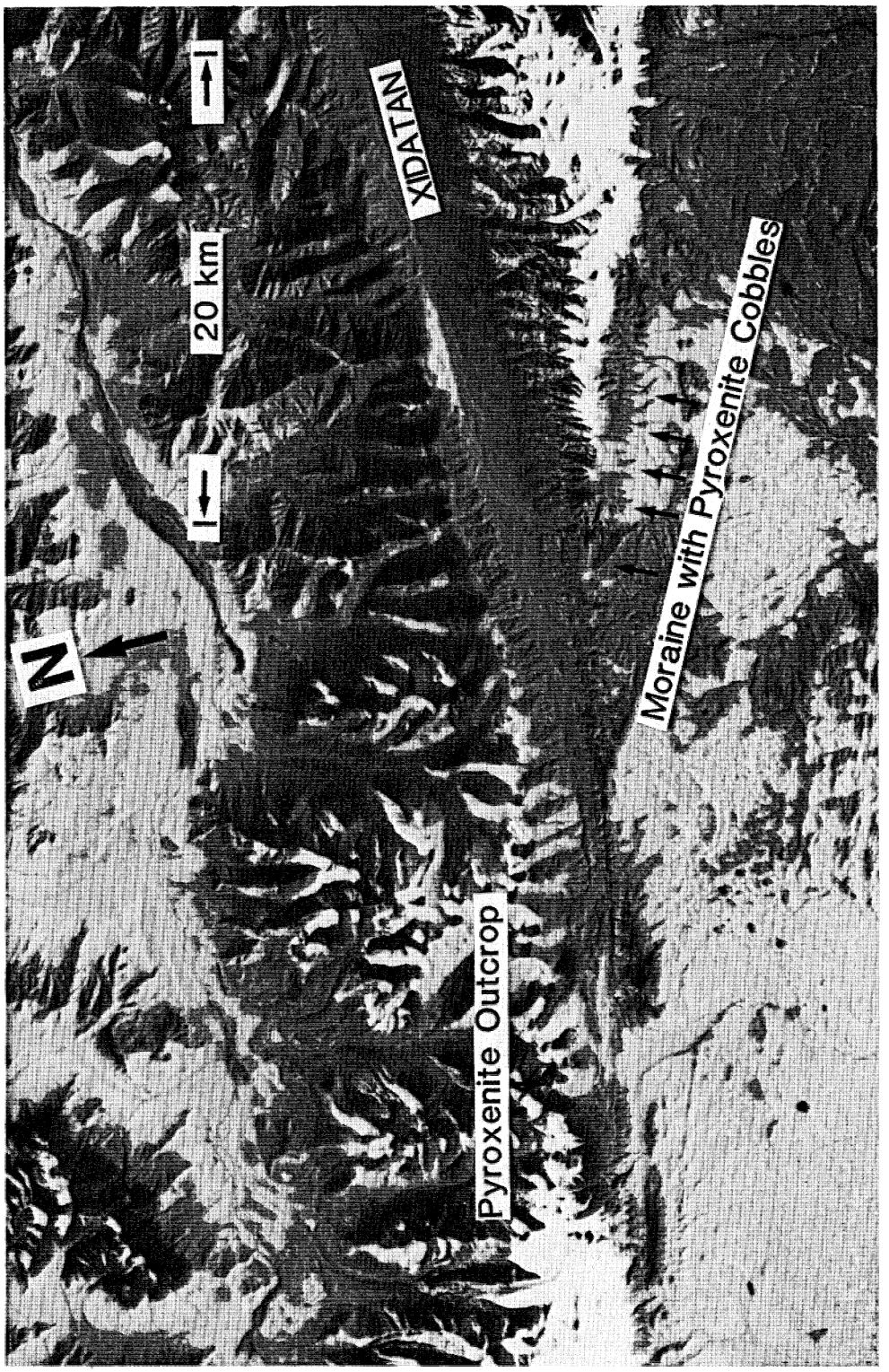

FIGURE 8. Large format camera photograph of the area where the Xidatan–Tuosuohu–Maqu and Kunlun Pass faults approach one another showing the locations of the outcrop of pyroxenite and the moraines containing pyroxenite cobbles.

in figure 2). They bound a northeast-trending valley, which appears to be a graben. Bedrock crops out in places in the valley, but most of its floor is covered by recent fluvial gravel, deposited by southwesterly-flowing rivers. Although there is an obvious vertical component of displacement on the edges of the valley, with the flanks of the valley standing several hundred metres above the valley floor, the relative importance of normal and strike-slip faulting cannot be evaluated easily from the satellite imagery. The fault plane solution of one earthquake, which occurred on 22 May 1971 east of Amdo (figure 1), indicates essentially pure strike-slip displacement with a left-lateral sense on the northeast-trending nodal plane (Molnar & Chen 1983).

We examined evidence for recent faulting at localities on both sides of this northeast-trending valley. On the south side of the valley, we saw no clear evidence of a recent fault scarp, but we examined only a short segment where the main road crosses the southern edge of the valley (C in figure 2). The unconsolidated cobbles and gravel exposed in the roadcut have been folded and thrust over one another (figure 3), similar to those observed in cross-sections across mole tracks and shutter ridges along the Xidatan–Tuosuohu–Maqu fault in the Kunlun, described below. Thus we infer that the deformation of these unconsolidated sediments is due to a large component of strike-slip, and not just normal, or reverse, faulting.

We examined the northern side of the valley near its western end (B in figure 2), where the north–south graben containing Tso Nag ends, and where Tertiary or Cretaceous redbeds crop out. In the mountains on the northern side of the valley, the redbeds dip steeply and are thrust southward over less consolidated conglomerates. Minor thrust faults are present in these poorly indurated sediments. In addition, the antecedent drainage of several rivers crossing this range and the incision of young alluvial fans on its south side suggest recent uplift of the range. Although we saw no clear recent scarp, the southern edge of the mountain range forms a relatively linear topographic front (B in figure 2), similar to but less impressive than that at the northern edge of the range on the south side of the valley. Moreover, an alignment of springs parallel to the front of the range suggests that a buried fault constitutes a groundwater barrier or a conduit for groundwater. These lines of evidence suggest that this deformation is very young.

The evidence for a component of thrust or reverse faulting is unequivocal, but we lack evidence constraining the proportion of strike-slip displacement. From the fault plane solution of the earthquake on 22 May 1971, from the linearity of the mountain front, and from small- and large-scale features seen in the range, we suspect that the strike-slip component is at least as large as the thrust component. In particular, small faults and slickensides almost subparallel to the southern margin commonly show a component of strike-slip displacement, dominantly of left-lateral sense. Also, the overall structure of the narrow range, with thrust faults dipping beneath both margins, is characteristic of compressional strike-slip zones ('flower structure').

North of the Tanggula, the pass where the road crosses from the province of Xizang to Qinghai, our route passed through a north–south valley a few km southwest of Wenquan (figure 1). At the southern end and on the west side of the part of the valley that we visited, hot springs emanate from an area with young, apparently Holocene, scarps with heights of several metres (figure 4). Beginning farther north on the west side of the valley, a recent scarp with about 1 m of displacement was clear along most of the part of the valley that we saw. The scarp is similar to, but smaller than, those on the west edges of the Gulu and Yangbajain grabens (see photos in Armijo *et al.* 1986 and Tapponnier *et al.* 1981*b*), and it probably reflects the

occurrence of an earthquake in the last few hundred years. In map view the scarp is not straight; it crosses small ridges and valleys on the east flank of the mountains that bound the valley in such a manner that if the fault is roughly planar, it dips eastward beneath the valley. Thus it is a normal fault, and the valley is a half-graben, or perhaps a graben, but we could see no evidence from the ground for young faulting on the east side of the valley.

This graben, north of the Tanggula, might be considered an extension of the Yangbajain–Gulu rift, mapped by Armijo *et al.* (1986). If the grabens are connected, however, the link between the northern end of the Yangbajain–Gulu system and the southern end of the Wenquan graben is not prominent on the satellite imagery of this regioin. Thus it seems possible that this graben, like most in northern Tibet, is more isolated from the others than the relatively continuous rift systems in southern Tibet.

We observed no other unequivocal evidence for recent faulting north of the Yangbajain graben and south of the Kunlun strike-slip fault system, over a distance of 250 km. A pair of nearly linear scarps in alluvial deposits can be seen on the Landsat imagery bounding a segment of the Tongtian River (a branch of the Jinsha or Yangtze) northeast of Wenquan, but we were unable to visit these scarps. The topographic maps show that their heights are about 10–20 m. They do not closely resemble the river terraces elsewhere along the river, and we suspect that they are young fault scarps. If so, they are the northernmost examples of normal faulting visible on the Landsat imagery near our route. Thus these features and the Wenquan graben mark a diminishing in importance of normal faulting northward.

South of Erdaogou, a prominent thrust fault (figure 1) was seen in outcrop carrying well-lithified Eocene red arenites southward over less consolidated marls and lake deposits of younger Tertiary age. Most of the displacement on this fault may be older than Quaternary, but some of it, at least, is probably very young. Southerly-flowing rivers from the interior of the Erdaogou ranges cut across the topographic barrier of the frontal range, and a small-scale incised meander was observed in a minor side stream in this frontal range, very close to the outcrop of the fault at the Lhasa–Golmud highway. The uplift implied by these drainage features is probably due to continued or renewed movement on the thrust fault. Moreover, obliquely-oriented slickensides in the Eocene arenites, like those in the redbed range near Amdo, indicate a component of strike-slip displacement.

This area and that near Amdo are among the few localities in the high plateau where a component of young reverse or thrust faulting can be reasonably inferred. Armijo *et al.* (in press) report another example several hundred km southwest, in clear association with strike-slip faulting. Although some workers might seize on these observations of reverse faulting as proof that crustal thickening is an important active process in Tibet, we consider it likely that the strike-slip components in these areas are comparable with the reverse components and unlikely that thrust faulting is widespread. Readers might recall that although the crust of the Basin and Range province in the western United States is undergoing horizontal extension by normal and strike-slip faulting, localized active thrust or reverse faulting also occurs within the province, such as at the east end of the Garlock strike-slip fault.

Major recent strike-slip faulting in the Kunlun

It is evident from the Landsat imagery and from satellite based photographs using the large format camera that, near the Lhasa–Golmud road, two major strike-slip faults, part of the Kunlun fault system, trend roughly east–west through the Kunlun Shan (figures 5, 9 and 10).

The northern of these faults, called the Xidatan fault by Chinese scientists, can be traced from several hundred km west of our traverse through the Xidatan ('western valley') and Dongdatan ('eastern valley'), where we worked extensively (figures 5, 9 and 10), and eastward several hundred kilometres through the lake Tuosuohu and the town of Maqu, where it is called the Maqu–Tuosuohu fault by Chinese scientists (e.g. Cui & Yang 1979; Li & Jia 1981) (figure 1). Left-lateral slip was inferred from adjacent structures seen on the Landsat imagery and from fault plane solutions of two earthquakes that occurred on it (Molnar & Tapponnier 1975; Tapponnier & Molnar 1977). One of those earthquakes, which occurred on 19 April 1963, was quite large: $M = 7.0$. Recent work by Cui & Yang (1979) showed numerous stream offsets and other features indicative of active left-lateral slip, and Li & Jia (1981) found a fresh rupture zone some 300 km in length with both vertical and left-lateral horizontal components of displacement reaching several metres near Maqu. Thus there is little doubt that the Xidatan–Tuosuohu–Maqu fault is a major, active, left-lateral strike-slip fault.

The second fault, the Kunlun Pass fault, is slightly oblique to the Xidatan–Tuosuohu–Maqu fault and follows the southern margin of the Burhan Budai mountains (figures 5, 6, 7, 8, 9 and 10). This fault can be traced on the satellite imagery east of the highway for about one hundred kilometres where it appears to curve southward (figures 5, 9, and 10) and where a component of thrust faulting should become increasingly significant. The average trend of the Kunlun Pass fault ($\approx 095°$) is slightly different from that ($\approx 090°$) of the Xidatan–Tuosuohu–Maqu fault. If projected west, the Kunlun Pass fault would intersect the Xidatan–Tuosuohu–Maqu fault just west of the west end of the Xidatan, approximately 25 km west of Kunlun Pass (figures 6 and 8). The fault trace disappears on both the Landsat imagery and the large format camera photos (figures 5 and 7) before intersecting the Xidatan–Tuosuohu–Maqu fault; it also proved impossible to trace the Kunlun Pass fault on the ground more than about 4 km west of the road.

The small- and large-scale geomorphology and the Quaternary offsets determined by us suggest that the Xidatan–Tuosuohu–Maqu fault is the major branch of the Kunlun fault system. The Kunlun Pass fault, while apparently having a substantial rate of movement in Holocene time, does not seem to have a large total offset. Landsat MSS images of the area crossed by the traverse and west of this area allow the main strand of the Kunlun fault to be followed as a clearly defined feature for 340 km west of the Xidatan, and it may continue as a less well defined array of splay faults, for about another 100 km to the southern margin of the Ayak Kum Köl basin. To the north of this main fault, another strand (not named) is almost as prominent on the Landsat images from 230 to 370 km west of the Kunlun Pass (figures 9 and 10), well to the west of the traverse line.

On the satellite imagery, this unnamed strand forms part of a zone of otherwise less continuous and/or oblique fault segments and splays and other linear features (figures 9 and 10). The discontinuous nature of this fault zone suggests that the overall displacement on it is small, at least compared with that on the main Xidatan–Tuosuohu–Maqu fault. It is likely, however, that there is some young displacement on these discontinuous faults and splays. Note that this zone lies west of the area where the main Xidatan–Tuosuohu–Maqu fault is transposed through a series of pull-apart basins and west of where the main fault undergoes a regional change in trend (figures 9 and 10). Thus it appears that this zone may have absorbed part of the slip on the eastern segment of the Xidatan–Tuosuohu–Maqu fault, and may continue to do so at the present time.

The traverse route approaches or crosses a few of these discontinuous faults and linear

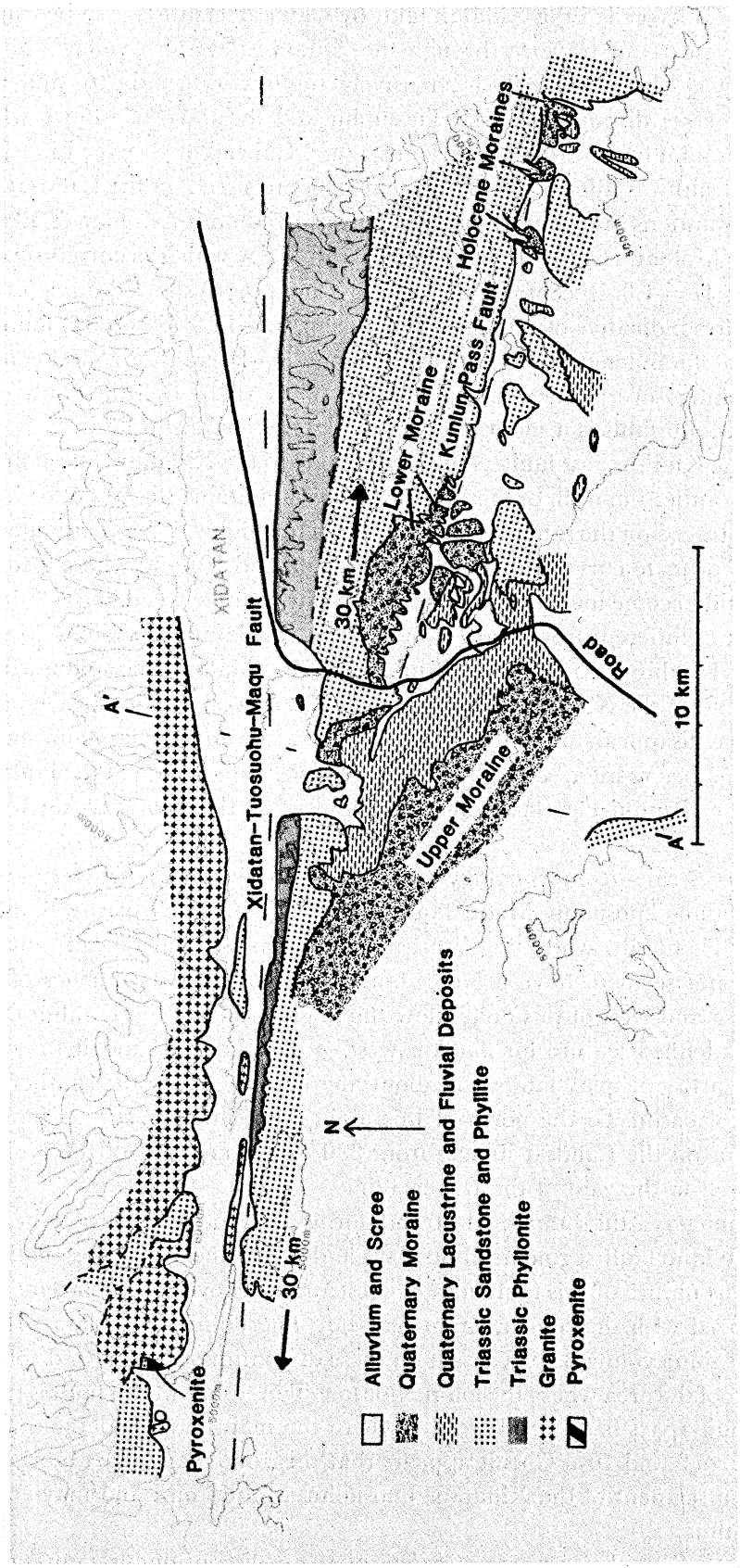

FIGURE 6. Geologic Map of Xidatan, Burhan Budai and Kunlun Pass region. The Burhan Budai consists mostly of Triassic sandstone, phyllite, and phyllonite, but on the ridge north of the Xidatan, granite crops out widely. South and west of the Burhan Budai a sequence of lacustrine deposits overlies alluvial deposits, which in turn overlie an older, lower moraine. This sequence is capped by a second, younger moraine. The lower, older moraine contains boulders of Triassic sandstone and phyllite, hornblende granite, gabbro, and pyroxenite. Pyroxenite was found in outcrop only to the west of the Xidatan, north of the fault. The distance between this outcrop and the easternmost exposure of moraine containing cobbles of pyroxenite is 30 km.

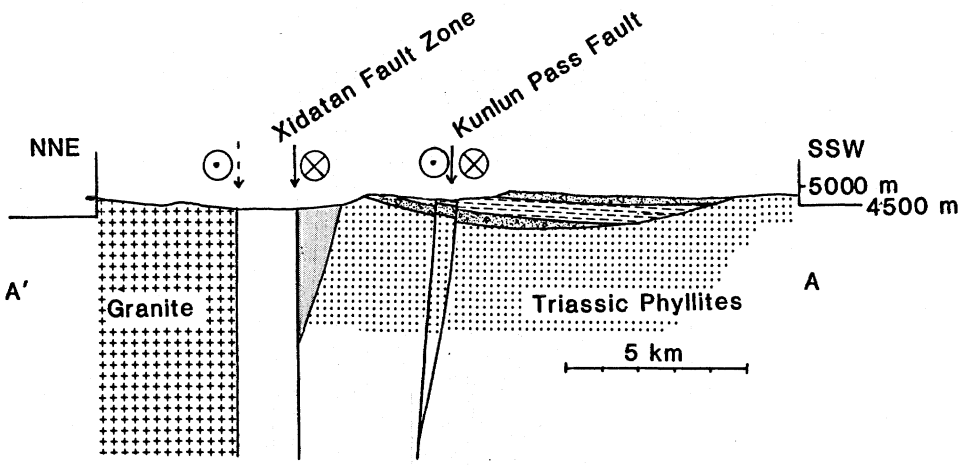

FIGURE 7. Geologic cross section across the Xidatan and lake beds just west of the Kunlun Pass, showing the two main strike-slip faults, the belt of phyllonite, and the lake beds. The extrapolation of rock units at depth is, of course, only tentative, and below the Xidatan no extrapolation of recent alluvial deposits was made. Symbols and location are those shown in figure 6.

features. In particular, the so-called North Kunlun faults (figures 9, 10 and 11), which separate the less deformed Carboniferous and volcanic rocks, lacking a cleavage, from strongly cleaved Ordovician and Permo-Triassic rocks to the south, appear to be part of this zone (see Coward *et al.*, this volume and Kidd *et al.*, this volume). The sense and amount of displacement along this contact zone is unknown, but from the observations noted above, it is possible that some displacement might be young and connected with the overall Kunlun fault system. The lack of prominent geomorphologic expression of the fault trace seen on the ground near the traverse suggests that any young displacement is likely to be small (not more than a few kilometres).

Our work focused on quantifying the rate of slip on the Xidatan–Tuosuohu–Maqu and Kunlun Pass faults and to a lesser extent on placing bounds on when the faults became active and on how recently slip might have occurred. Both because of its greater significance and its greater accessibility, the Xidatan–Tuosuohu–Maqu fault received more of our attention. We obtained an approximate average rate of slip for the Quaternary period and impressions both of when the last major earthquake occurred and how much slip can be associated with it. For the Kunlun Pass fault, we estimated an average slip-rate for Holocene time and a possible bound for the date of initiation of slip. We first discuss constraints on the displacement during Quaternary time and the age of initiation of the faults. Next we discuss Holocene displacements and average rates for the last 10,000 years, and then the evidence for recent offsets.

Quaternary offset and average slip-rate on the Xidatan–Tuosuohu–Maqu fault

As was described by Kidd *et al.*, this volume, and Smith & Xu, this volume, a relatively thick sequence of Quaternary deposits can be seen in the area around the Kunlun Pass and on the south slope of the Burhan Budai mountains (figures 6, 7, and 8). The oldest of these deposits appear to be ground moraine–unsorted, angular fragments, from sand-size to boulders, of Triassic sandstone and phyllite, granite, hornblende gabbro, and pyroxenite. These deposits seem to lie directly on green Triassic sandstone and phyllite. Overlying the moraine is alluvial gravel, in which an imbrication of pebbles implies a southerly direction of flow. This gravel, in turn, is overlain by fine sand, silt and clay deposited in a lake and by interbedded alluvial

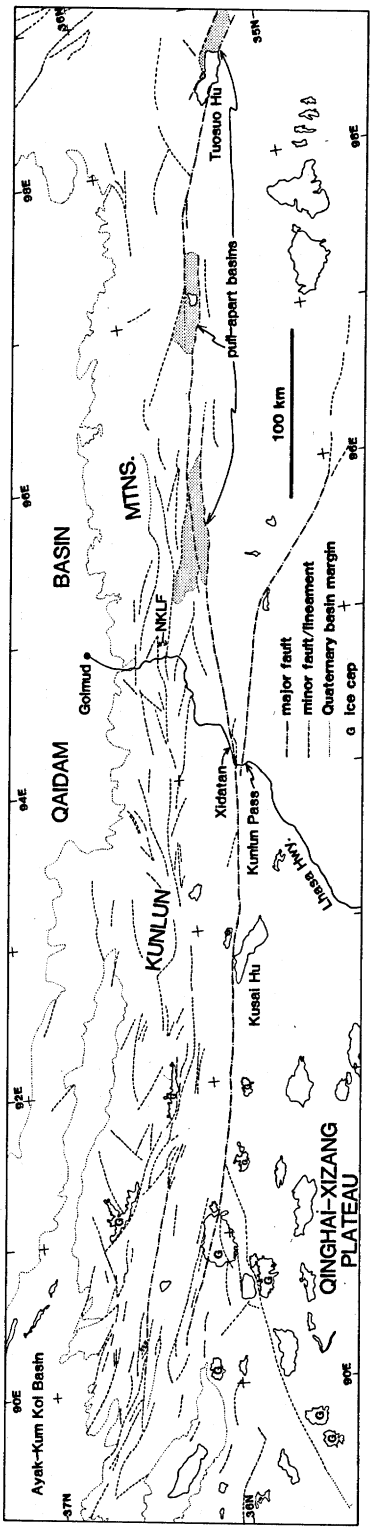

FIGURE 9. Sketch map of the western part of the Kunlun fault system with the main and subsidiary fault strands identified from satellite imagery. The 'North Kunlun Faults' (NKLF) appear to be subsidiary faults. See text for details.

FIGURE 10. Mosaic of three Landsat images covering a portion of the western reaches of the Kunlun fault system. The main Xidatan–Tuosuohu–Maqu fault extends from about 90.5° E to 95° E on this mosaic. The traverse line crosses this fault in the Xidatan, near Kunlun Pass (see figure 9 to locate the mosaic). The minor faults and linear features identified in the area of the mosaic are indicated on figure 9. Locations of possible offset continuations of the phyllonite unit identified on these images are shown on figure 11.

(*Facing p.* 346)

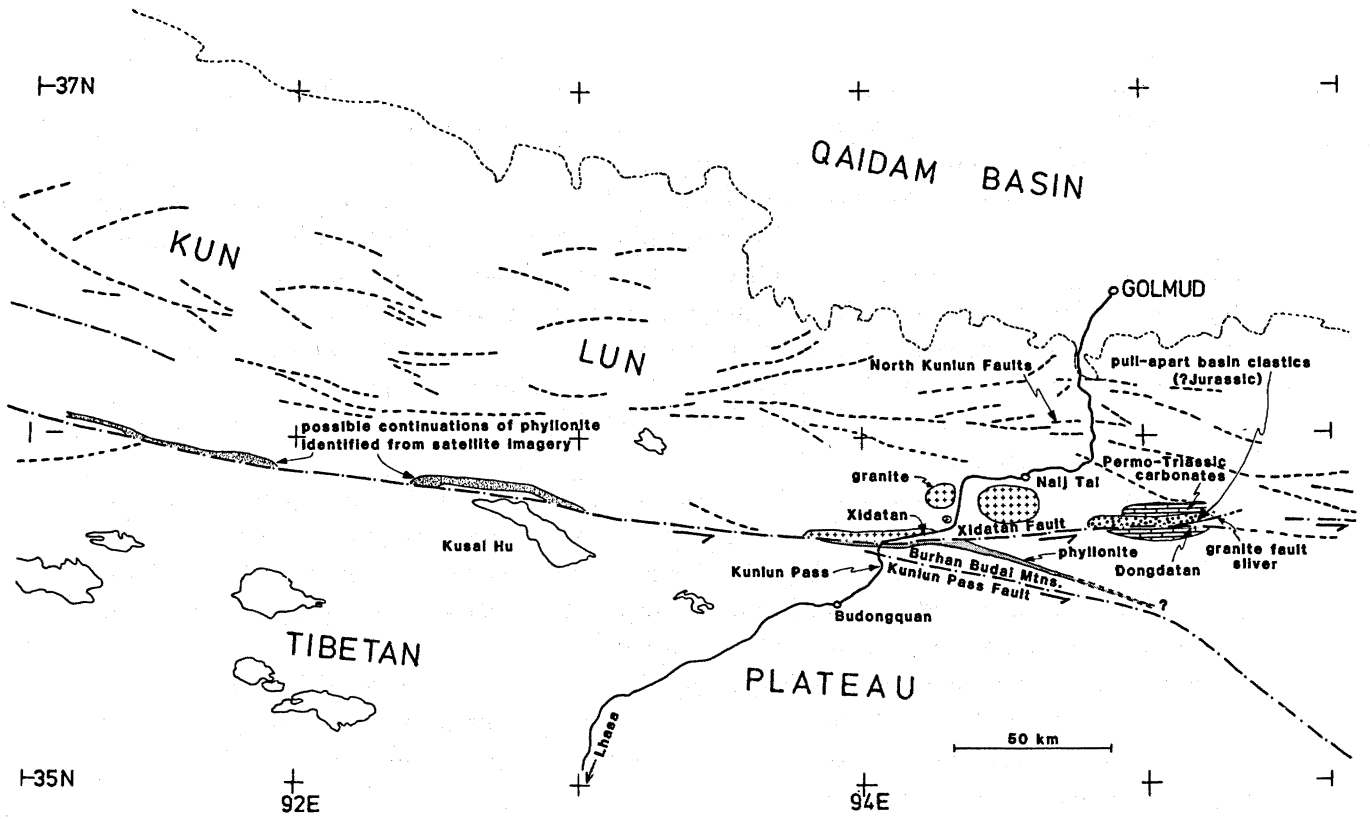

FIGURE 11. Sketch map of a portion of the Kunlun fault system showing possible offset segments of the phyllonite unit that is seen truncated just west of the Kunlun Pass region. The Dongdatan pull-apart sequence (?Jurassic) is shown together with known areas of granite and carbonate rocks adjacent to the Xidatan–Tuosuohu–Maqu fault.

sand. This relatively thick sequence, 100–200 m, is overlain by ground moraine consisting largely of blocks of Triassic(?) sandstone and phyllite with some granite clasts. The entire sequence dips roughly south at 10° to 15° (figure 7).

We, like Wu *et al.* (1982), infer a southward flow of the glaciers that deposited both moraines. This inference derives principally from the imbrication of the pebbles in the intervening layer of alluvial gravel. In addition, however, we saw no granite outcrops in this area except north of the Xidatan, implying that the blocks of granite in the moraines were derived from the north.

As Wu *et al.* (1982) pointed out, a northern source requires that the Xidatan, a valley more than 1000 m deep (figure 6), be younger than the moraines, which are perched on the surrounding mountains. The linear configuration of the Xidatan, parallel to the Xidatan–Tuosuohu–Maqu fault, suggests that its existence is due to slip on that fault, possibly with a small component of extension across it. Although valley glaciers with terminal moraines are present in the valleys high in the Burhan Budai, no clear moraines were seen within the Xidatan. Moreover, hanging valleys, typical of the sides of deep glacially eroded valleys, also were not seen along the Xidatan. Thus we infer that the Xidatan did not form by glacial erosion. Wu *et al.* (1982) inferred that slip on the fault began after the lake beds and the moraine covering them were deposited, an inference with which we do not concur; nevertheless, the formation of the valley probably is quite young (latest Pliocene at the oldest).

Most of the boulders in the older moraine, and all of those in the younger moraine, could have been derived from nearby sources. Triassic green sandstone and phyllite abound throughout the Burhan Budai, and granite crops out widely along the northern edge of the Xidatan. Finding gabbro and especially pyroxenite in the older moraine, however, was a surprise, and with left-lateral strike-slip faulting in mind, we sought a source west of the moraine in which boulders of them had been found. Both gabbro and pyroxenite were found cropping out only in a small area adjacent to Triassic schist at the western end of the granite, which borders the Xidatan (figure 6), as Wu *et al.* (1982) had already found, unbeknownst to us at that time. We infer that the boulders in the moraine near the Kunlun Pass were derived from this small outcrop (or, if not, from another source farther west, too far for us to visit). The distance from this outcrop to the eastern end of the moraine where pyroxenite boulders are present is about 30 km. Thus, 30 km (or more) of left-lateral slip seems to have occurred since the moraine was deposited.

We cannot eliminate completely the possibility that a glacier flowed east from the pyroxenite outcrop to the moraine, but we doubt this strongly. First, we did not see the moraine farther west than that shown on the map (figure 6) and therefore closer than 20 km to the pyroxenite outcrop. Second, the imbrication in the pebbles directly overlying the lower moraine indicates a direction of transport toward the south, not the east. Third, the lack of evidence for glaciation within the Xidatan is consistent with that valley being formed by tectonic, and not by glacial, processes. Thus, although none of these arguments proves that the glaciers that deposited the pyroxenite flowed south a few kilometres instead of east many tens of kilometres, we consider this latter possibility very unlikely.

The age of the older moraine is probably not older than late Pliocene, or approximately 2.4 Ma, when ice-rafted material was first deposited in abundance in the Atlantic Ocean (Shackleton *et al.* 1984) and when glaciation first became widespread in Europe and North America (e.g. Holmes 1965). Qian *et al.* (1982) investigated the magnetostratigraphy of the lake bed sequence and inferred an extrapolated age for the older moraine of 2.8 Ma. The sparse sampling in the lake beds and the imperfect correlation of reversals with the geomagnetic reversal time scale make their inferred ages quite uncertain, and it seems remotely possible to us that the age of the older moraine is as young as 1.5 Ma. Thus we conclude that average rate of slip during the Quaternary period has been at least 10 mm/a, probably closer to 13 mm/a if the age of the moraine is 2.4 Ma, and possibly as much as 20 mm/a.

Total offset and age of displacement on the Xidatan–Tuosuohu–Maqu fault

A large-scale, low-angle truncation of a thick phyllonite unit (discussed by Kidd *et al.*, this volume) was observed on the south side of the Xidatan–Tuosuohu–Maqu fault 20 km WNW of the Kunlun Pass (figures 6, 11, and 12). The phyllonite, because of its prominent phyllitic muscovite foliation, is a very distinctive lithologic unit, and, when seen at a distance in the field, contrasts strongly with adjacent green phyllitic Triassic arenites and slates. This contrast is also clearly distinguishable on the unenhanced Landsat MSS image of the area. The bluish-white tone of the phyllonite unit on the image is also distinct from both of the other light-toned rock units in the vicinity, and in particular from the pinkish-tan tone of granitic rocks, which occur along the western part of the north side of the Xidatan, as well as from the tan tone of Permo-Triassic carbonates seen on the north and south sides of the Dongdatan (figure 11).

Given that substantial left-lateral slip has occurred across the Kunlun fault system, the offset

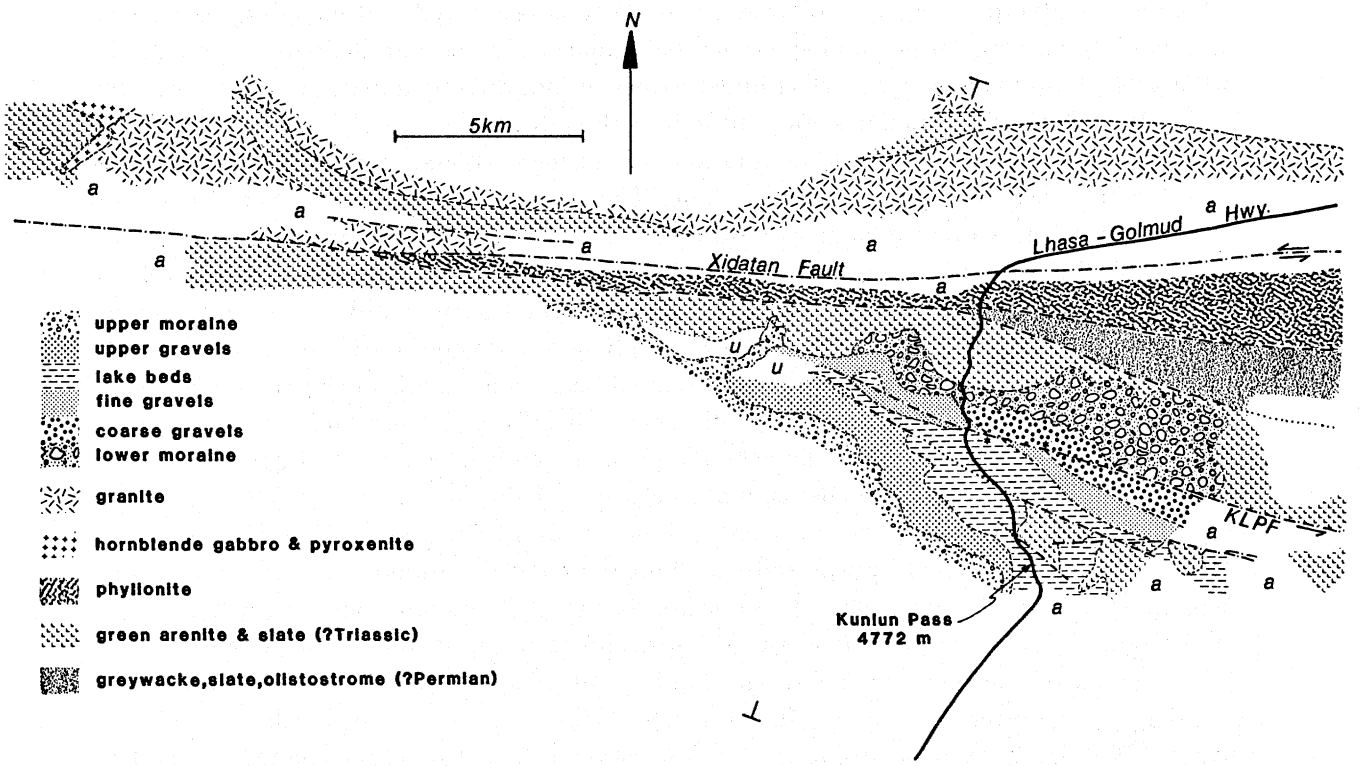

FIGURE 12. Geological map of bedrock in the Kunlun Pass region, showing the possible total offset on the Kunlun Pass fault (KLPF); the contact of lower coarse and fine gravel units is truncated by the fault at points marked with asterisks. Ends of the cross section (figure 7) are marked by Ts; u – undifferentiated Pleistocene sequence; a – Alluvium; blank – unmapped; dash-dot lines – faults, dotted where uncertain or imprecisely located.

continuation of the phyllonite should be found west of the Kunlun Pass region, on the north side of the fault. On the Landsat images, a pale unit, which more closely resembles the phyllonite in tone that it does known granite or limestone, is first seen on the north side of the main strand of the Kunlun fault system (Xidatan–Tuosuohu–Maqu fault) 75 km west of the truncation of the phyllonite observed in the field (figure 11). If this pale unit is the phyllonite, and not limestone or marble, then the minimum total offset of the main (Xidatan) strand of the Kunlun fault system is 75 km. At the rates of displacement deduced by us from Quaternary offsets, this total displacement would have accumulated in no more than about 7 Ma.

The total offset could be more, perhaps by a substantial amount, than the 75 km deduced above. First, south of the Xidatan, the southern side of the phyllonite is in sharp, subvertical fault contact, involving brittle deformation, with either the green Triassic arenites and phyllitic slates or with a sliver of Permian(?) greywackes, slates, and local olistostromes. This fault is also a sinistral strike-slip structure presumed to be related to the present Kunlun fault system, but not a currently active strand and with an unknown total displacement.

Second, the proposed offset continuation of the phyllonite seen on the images is truncated against the north side of the main Kunlun fault strand in three places, not just one (figure 11), making it less certain which should be matched with the truncation on the south side. Given the uncertainties, we suggest that the 75 km offset may be only a minimum total offset for the main strand (Xidatan–Tuosuohu–Maqu fault) of the Kunlun fault system.

In the Dongdatan, a sequence of arenaceous clastics, locally red and including minor coal beds, lies in a narrow, largely fault-bounded belt adjacent to and parallel with the north side of the present fault valley. This well-lithified sequence (not directly dated) lies unconformably on the Permo-Triassic carbonates adjacent to it. Although it is moderately folded, it must have been deposited after the main folding and foliation of the carbonates, an event that we think occurred in late Triassic to mid-Jurassic time. The present geometry, facies, and structural relationships of this sequence suggest that it represents a deformed pull-apart basin on a strike-slip fault. While it could be relatively young (Miocene, for example), it could alternatively be as old as Jurassic; coal containing a possibly Mesozoic plant fossil (Smith & Xu, this volume) occurs in a minuscule fault sliver adjoining the phyllonite on the south side of the Xidatan (figure 11) and perhaps came from this or a related basin. The significance of this sequence of rocks is that it suggests that some of the displacement on the Kunlun fault system could be relatively old (Mesozoic) and unrelated to the present tectonics. The overall geometry of this possible pull-apart structure suggests that the sense of displacement was left-lateral, but confirming evidence for this was not seen in the rocks from that pull-apart basin.

The deformation implied by a prominent change in the orientation of the ductile stretching lineation (Coward *et al.*, this volume), as one approaches the Xidatan from the north along the main Golmud–Llasa highway, does suggest Jurassic strike-slip displacement along the zone now occupied by the Xidatan–Tuosuohu–Maqu fault. North of the present fault valley, the lineation plunges steeply; coming towards the Xidatan, it progressively changes, over a distance of about 2 km, to a sub-horizontal attitude, and the nature of the change implies left-lateral offset. This deformation, unlike the other evidence for strike-slip faulting discussed above, involved ductile strain at depths of at least several kilometres; nevertheless, any offsets of lithic units produced by it will contribute to the total offset and complicate the determination of the offset resulting from the collision of India with Asia.

The southern margin of this probable pull-apart basin sequence, which forms the northern edge of the Dongdatan Valley, has a sliver of chloritised and densely fractured granitic rock faulted against it (figure 11). While no feature was seen in this badly altered rock to connect it conclusively with other granitoid rocks observed to the west, the nearest outcrop of granitic rock that is immediately adjacent to the Xidatan–Tuosuohu–Maqu fault is about 90 km to the west in the Xidatan. At present, we do not attach much significance to this possible offset because the rocks need not be from the same body. If it is a real offset, however, this distance is not likely to be a total offset because both occurrences are on the north side of the main (Xidatan–Tuosuohu–Maqu) fault strand.

Holocene slip on the Kunlun Pass fault

As described above, the Kunlun strike-slip fault system consists of two strands. The Xidatan–Tuosuohu–Maqu fault is the major one of the two. The Kunlun Pass fault lies south of it and strikes at an acute angle to it, and they approach one another just west of the Kunlun Pass (figures 5, 6, 12, and 13). We studied a segment of the Kunlun Pass fault extending east from the main road for about 25 km. West of the road this fault was not very clear, and we could not trace it with confidence. Thus we gained little insight into how the two faults intersect, or interact.

The Kunlun Pass fault is very clearly defined both on the satellite imagery (figures 5 and 14) and on the contour maps provided to us (figures 6 and 13). It follows the foot of the Burhan

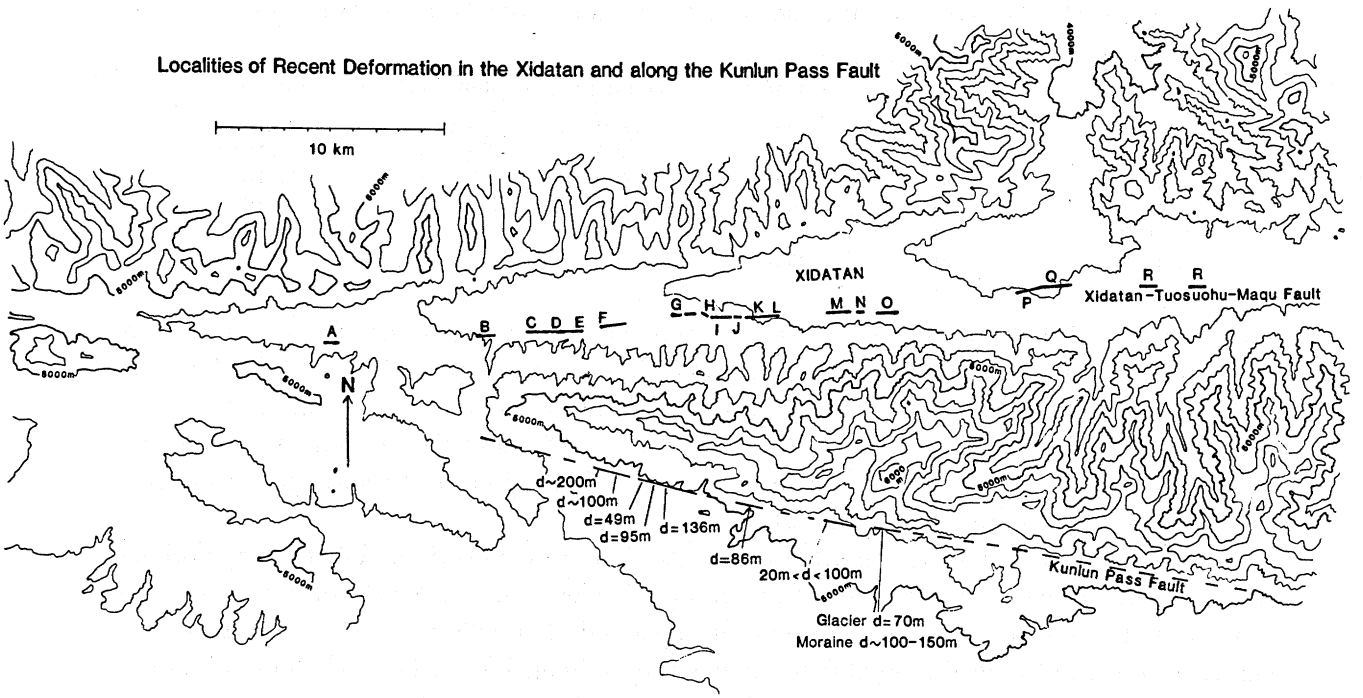

FIGURE 13. Map showing localities of clear offsets (d) on the Kunlun Pass fault (see also table 1) and areas of disruption along the Xidatan–Tuosuohu–Maqu fault in the Xidatan. Letters indicate areas discussed in the text.

Budai mountains on their southern side at the break in slope. The fault is also very clear from the ground, for it displaces most small streams that cross the fault (figures 15 and 16). We did not see, however, features clearly offset only a few metres by slip on the fault or other evidence of recent deformation, such as tension gashes or mole tracks, that might be associated with a recent moderate or large earthquake.

The offset streams demonstrate clear left-lateral slip, which probably has occurred during Holocene time, or at least since the last glaciation. Virtually all streams with length of 1 km or more are displaced. The measured amounts of displacement vary from 49 m to 135 m and possibly to 200 m. In some cases it is difficult to distinguish offset due to faulting from other bends in streams or possible stream capture. In such cases we include large uncertainties in our estimates of the offsets. In other cases, V-shaped valleys are clearly displaced as the streams debouch onto their alluvial fans south of the fault (figures 15 and 16).

The amount of offset is clearly larger for longer streams and for deeper valleys. In all but one case we measured offsets using a tape measure. In that one exception we paced the offset. There was insufficient time to make detailed contour maps. Using the topographic maps we measured the lengths (l) of the V-shaped valleys of the streams with clear offsets and their maximum widths (w) and depths (h), where the streams reached the fault. These quantities, plus estimates of the volume of material eroded ($V \approx 1/6\, l \cdot w \cdot h$) and of the area of the drainage basin ($A \approx 1/2\, l \cdot w$), are listed with the measured offsets in table 1. The locations of the streams are identified on figure 13 by the measured offsets.

The volume of the material eroded divided by the area of the drainage basin ($V/A \approx 1/3\, h$) equals the product of the average erosion rate and the duration of incision. Thus, if both the

TABLE 1. OFFSETS AND DIMENSIONS OF VALLEYS BY THE KUNLUN PASS FAULT

offset/m	maximum depth/m	maximum width/m	length/m	volume/m^3	area of drainage basin/m^2
136 ± 10	120	400	1200	9.6×10^6	2.4×10^5
95 ± 6	100	400	900	6.0×10^6	1.8×10^5
49 ± 4	50	400	600	2.0×10^6	1.2×10^5
86 ± 10	80	600	800	6.4×10^6	2.4×10^5
100^{+100}_{-50}	60	500	1800	9.0×10^6	4.5×10^5
200 ± 50	40	300	1000	2.0×10^6	1.5×10^5

erosion rate and the slip rate were constant when averaged over periods of a thousand years or so, then the amounts of offset should be proportional to the depths of the valleys. A plot of V/A vs. d (displacement) does yield a linear relationship if one ignores one offset of dubious certainty (figure 17). The inferred slip rate would be 3.2 times the erosion rate. Thus, an estimate for the erosion rate would yield an estimate of the slip rate, or conversely a slip rate of 10 mm/a would imply denudation at 3 mm/a.

We are not aware of any attempts to estimate erosion rates in northern Tibet, to say nothing of the small drainage basins in the Burhan Budai. Nevertheless, a rate of 3 mm/a seems reasonable to us in the climatic conditions at an elevation of 5000 m for erosion of relatively thinly bedded sandstone and phyllite in small, steep drainage basins. Plots of denudation rates vs. the areas of drainage basins in the midwestern United States (Brune 1948) indicate an overall tendency for the rates to decrease proportionally to the 0.15 power of the area (Langbein & Schumm 1958). Schumm (1963) concluded that the mean denudation rate for a basin of about 3800 km^2 (1500 sq. mi.) is about 1 mm/a. An extrapolation of this to basins with areas of 0.1 to 0.4 km^2 yields denudation rates of 4.0 to 4.9 mm/a. Although this extrapolation for different climatic conditions and different rock types cannot be used to predict accurate denudation rates, it does indicate that erosion rates of a few mm/a are not unreasonable.

We cannot determine accurate ages of these valleys or the rate of slip, but three observations suggest a Holocene age and hence a slip-rate of about 10 mm/a. First, the valleys are more nearly V-shaped than U-shaped in cross section (figures 15 and 16), and therefore they do not appear to be glacial in origin. Second, there are no terminal moraines in front of these small streams. The existence of active glaciers in neighbouring valleys, however, makes it virtually certain that there was glaciation in the Burhan Budai and probably a glacial maximum in the last 18,000 years, as there was elsewhere in the world. Thus these valleys are probably post-glacial in age. Third, at present one glacier crosses the fault, and indeed the eastern edge of that south-flowing glacier is offset 70 m left-laterally (figures 14 and 18). The glacier is receding, and much of its terminal and lateral moraines are preserved. The eastern edges of these moraines lie 100 to 150 m east of the eastern edge of the glacial valley north of the fault and through which the ice flows. The age of this moraine is probably also Holocene or very late Pleistocene (less than 18,000 years).

The assignment of a Holocene age to features displaced approximately 100 m yields an average slip rate of about 10 mm/a. Clearly this estimate is quite uncertain, and a range from 5 to 20 mm/a is probably allowed by the varying amounts of offset and the uncertainty in the ages for when incision began. Nevertheless, it is important to note that the average Holocene slip rate on the secondary fault in the Kunlun fault system is at least several mm/a. Clearly this fault also is a major one.

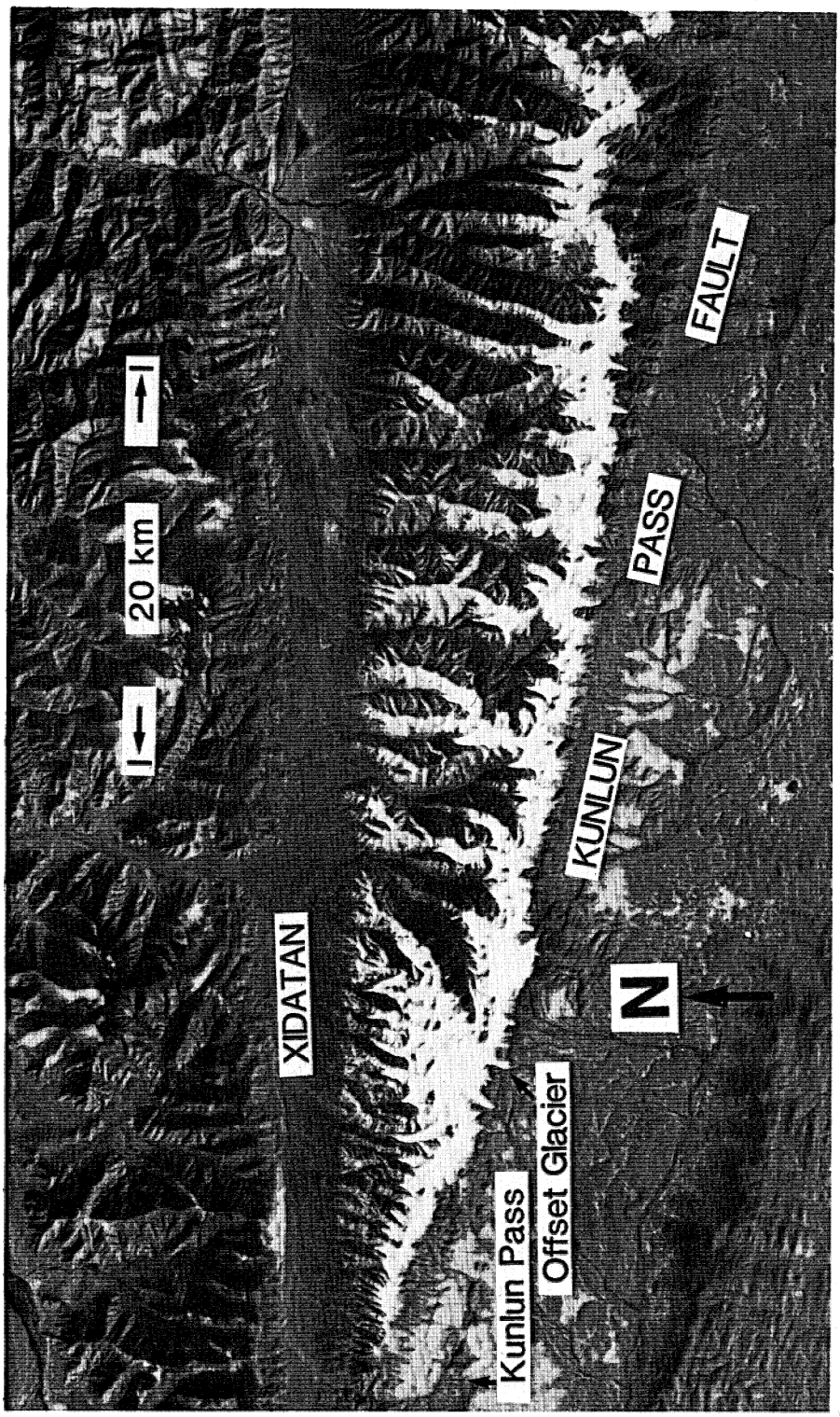

FIGURE 14. Large format camera photograph of the Kunlun Pass fault, showing the clear topographic expression of the fault and the location of the offset glacier (figure 18).

(*Facing p.* 352)

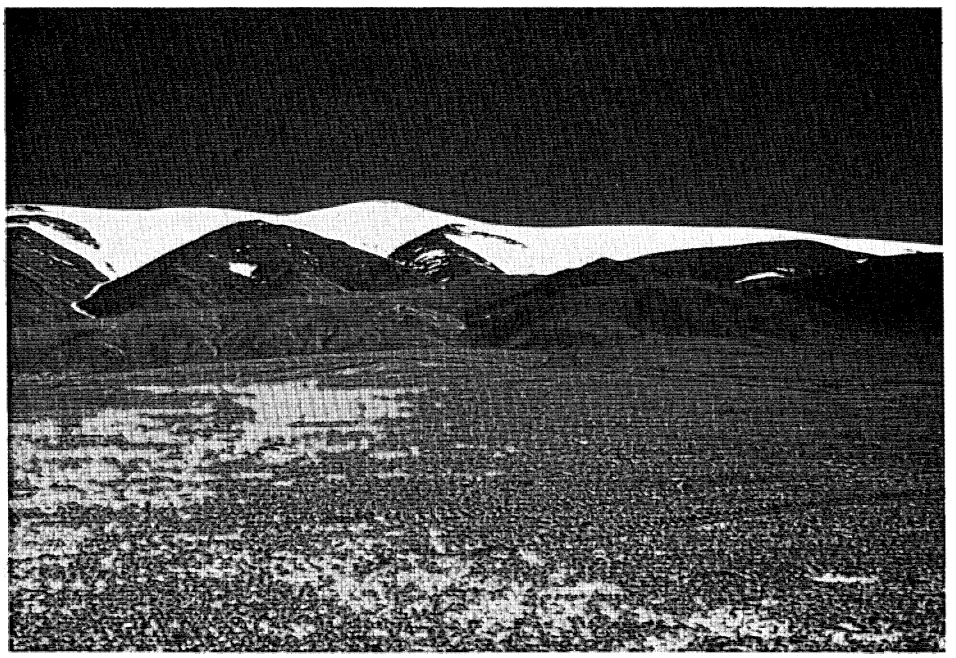

FIGURE 15. Photo looking north at an offset stream along the Kunlun Pass fault. The stream in the valley in the centre of the photo flows toward the photographer, but at the foot of the nearer hills it is displaced to the right (east) 49 ± 4 m.

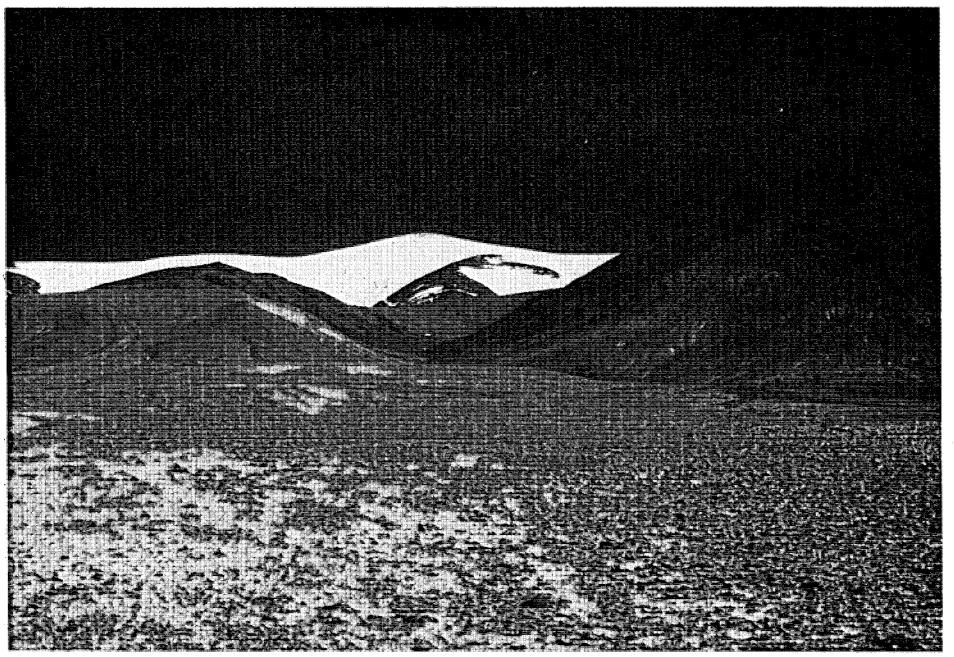

FIGURE 16. Photo looking north at a second offset stream along the Kunlun Pass fault. The valley in the centre of the photo is the same one shown on the right edge of the photo in figure 15. Again the stream flows directly toward the photographer but is offset at the Kunlun Pass fault, at the foot of the hills. The amount of offset is 95 ± 6 m.

FIGURE 18. Photo looking north at a major glacier flowing south from the highest peak in the Burhan Budai. Where the glacier reaches the Kunlun Pass fault at the foot of the mountains, it is offset about 70 m (see also figure 14). The terminal moraine of the receding glacier is offset between 100 and 150 m. Since this moraine probably was left by the last glaciation some 10 ka to 18 ka, the average rate of slip during Holocene time probably has been about 10 mm/a.

FIGURE 19. Photo looking west along the Xidatan–Tuosuohu–Maqu fault in its western segment near D in figure 13. The dark linear zone in the middle foreground is a tension gash obliquely crossing a shutter ridge that recedes from the photographer. Sag ponds farther in the distance have formed by segments of shutter ridges blocking the northerly-flowing streams.

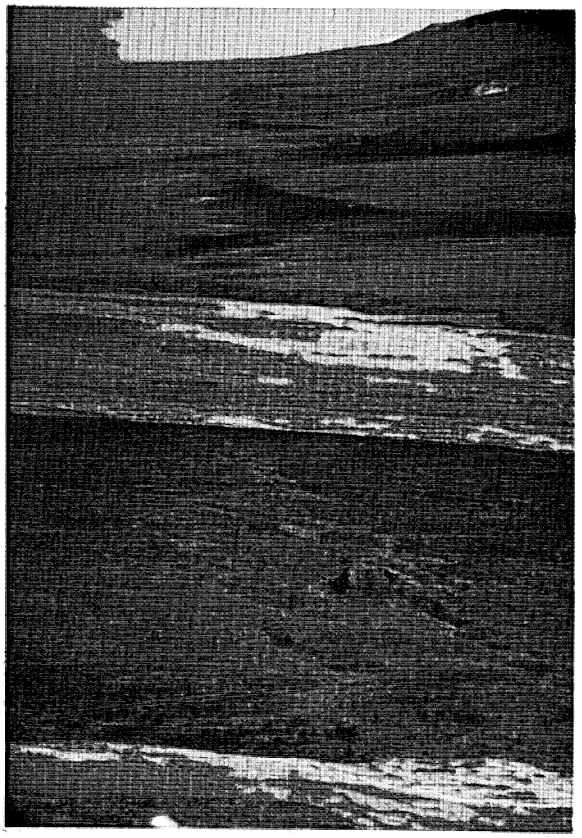

FIGURE 20. Photo (taken with a lens with a focal length of 135 mm) looking west along the Xidatan–Tuosuohu–Maqu fault from a hill near the locality I in figure 13. Streams in the foreground and the middle of the photo have obliterated evidence of surface faulting. Between the streams a small man-made hill lies within a zone of large tension gashes that trend northeast–southwest (see figure 21). In the distance, the fault has formed a ground-water barrier that is manifested by dark areas of more lush vegetation than on the neighbouring alluvial fans.

FIGURE 21. Photo taken from the man-made hill shown in figure 20 and looking east along the Xidatan–Tuosuohu–Maqu fault (J in figure 13). Doyle Watts is shown standing in a large tension gash, which trends northeast–southwest. The depth is nearly 2 m. As in figure 20, the fault is defined clearly by the darker vegetation growing on and adjacent to it in the distance.

FIGURE 24. Photo looking north-northwest at a small offset of a small stream gully. The gully entering the photo on the left trends north and is offset about 10 ± 2 m before reaching a wide braided stream. This locality is labelled V in figure 23.

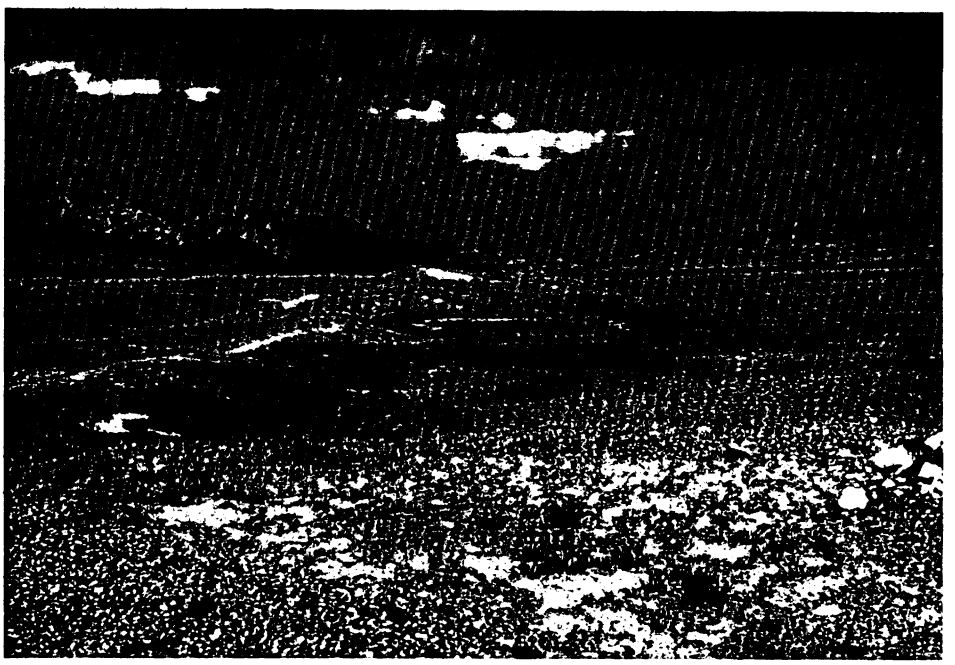

FIGURE 25. Photo looking east along the Xidatan–Tuosuohu–Maqu fault and showing sag ponds and a shutter ridge in the Dongdatan (W in figure 23). Drainage from the south (right) is blocked by the shutter ridge that recedes from the left lower edge of the photo across and away to the middle of the photo. A dry sag pond in the middle of the photo is about 20 m wide. The height of the shutter ridge is as much as 5 m higher than the dry bottom of the sag pond.

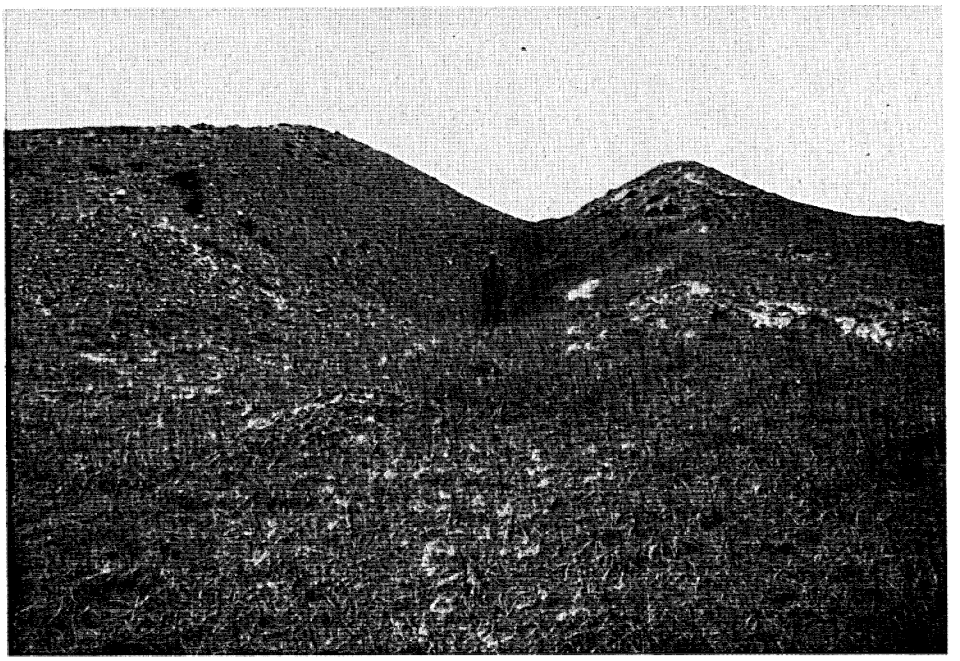

FIGURE 26. Photo looking southwest toward a huge tension gash within a high shutter ridge in the Dongdatan (W in figure 23). Michael Ward, standing in the tension gash, stands about 180 cm tall.

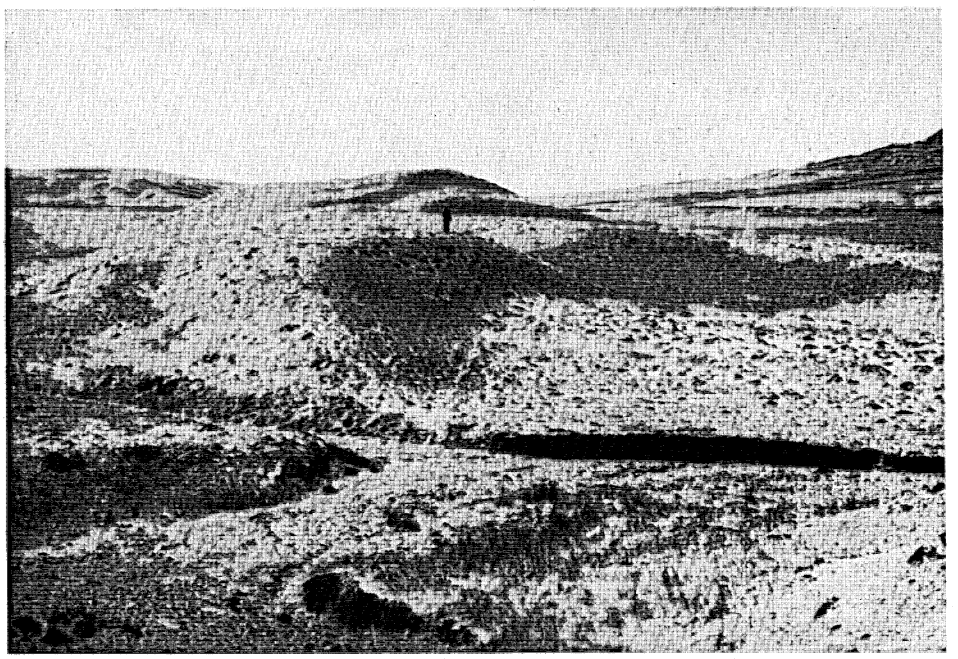

FIGURE 27. Photo looking west along the shutter ridge and the escarpment where the contour map in figure 28 was made. Two north-flowing streams join in the foreground where they cross the fault. Bill Kidd stands just south of (to the left of) a large area in which stream cobbles are exposed in groups. These cobbles apparently were deposited by the stream in the foreground when the flat area once lay closer to the photographer.

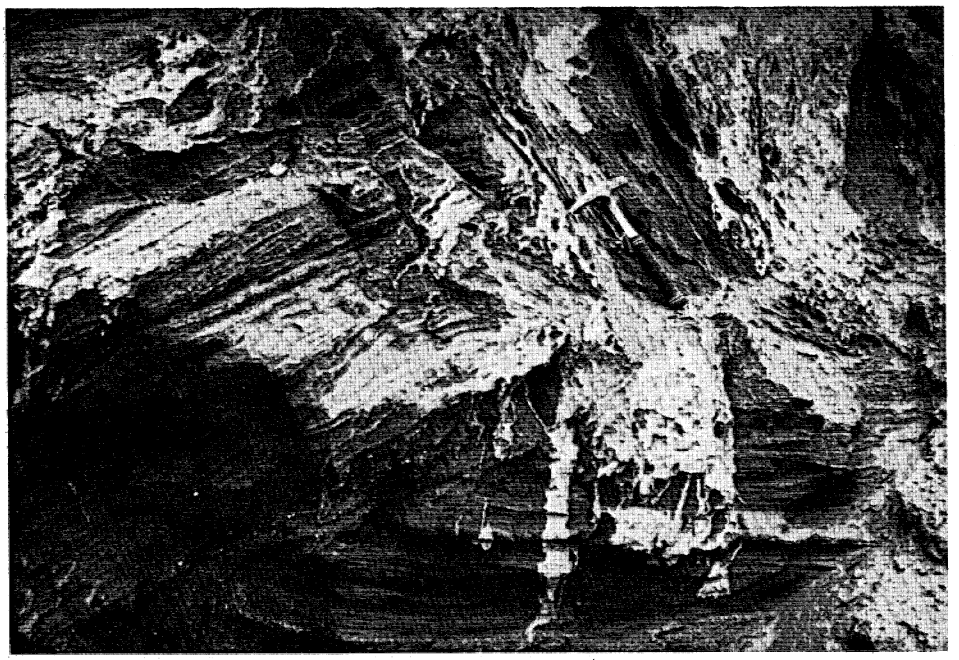

FIGURE 29. Photo, looking east, of a small thrust fault in sand and gravel deposited within the fault zone in the Dongdatan (Y in figure 23) and deformed by the formation of a shutter ridge.

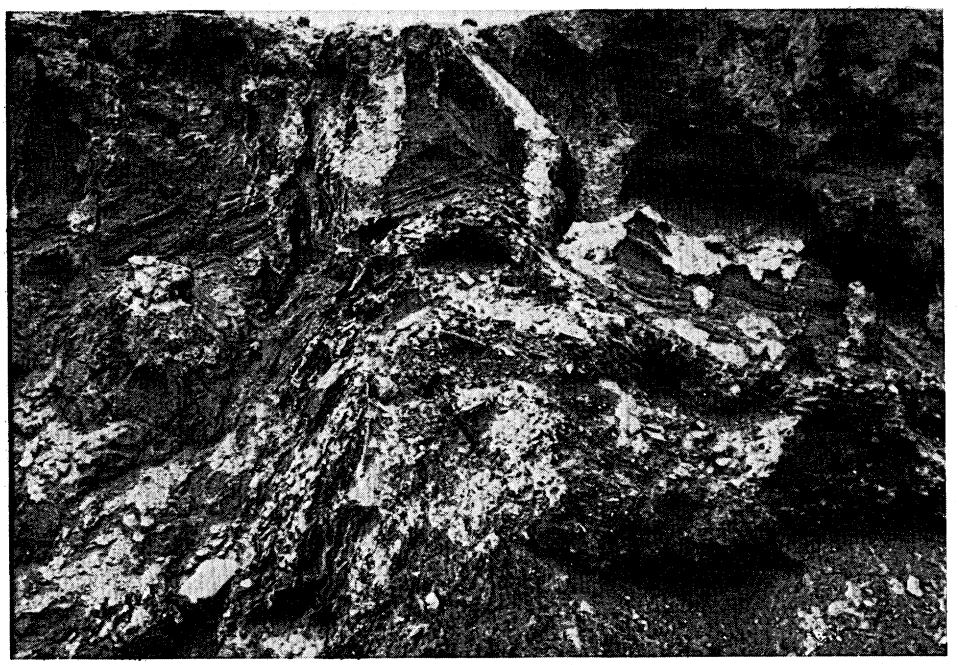

FIGURE 30. Photo, looking east, of a small fold in stream gravels within a shutter ridge in the Dongdatan (Y in figure 23). The hammer in the centre of the photo gives a scale; the gravel is folded into an overturned fold with a steep northern flank. Left of the hammer the gravel beds dip nearly vertically, but to the right they are nearly flat. The overlying sand reveals the same folding but less clearly than the gravel.

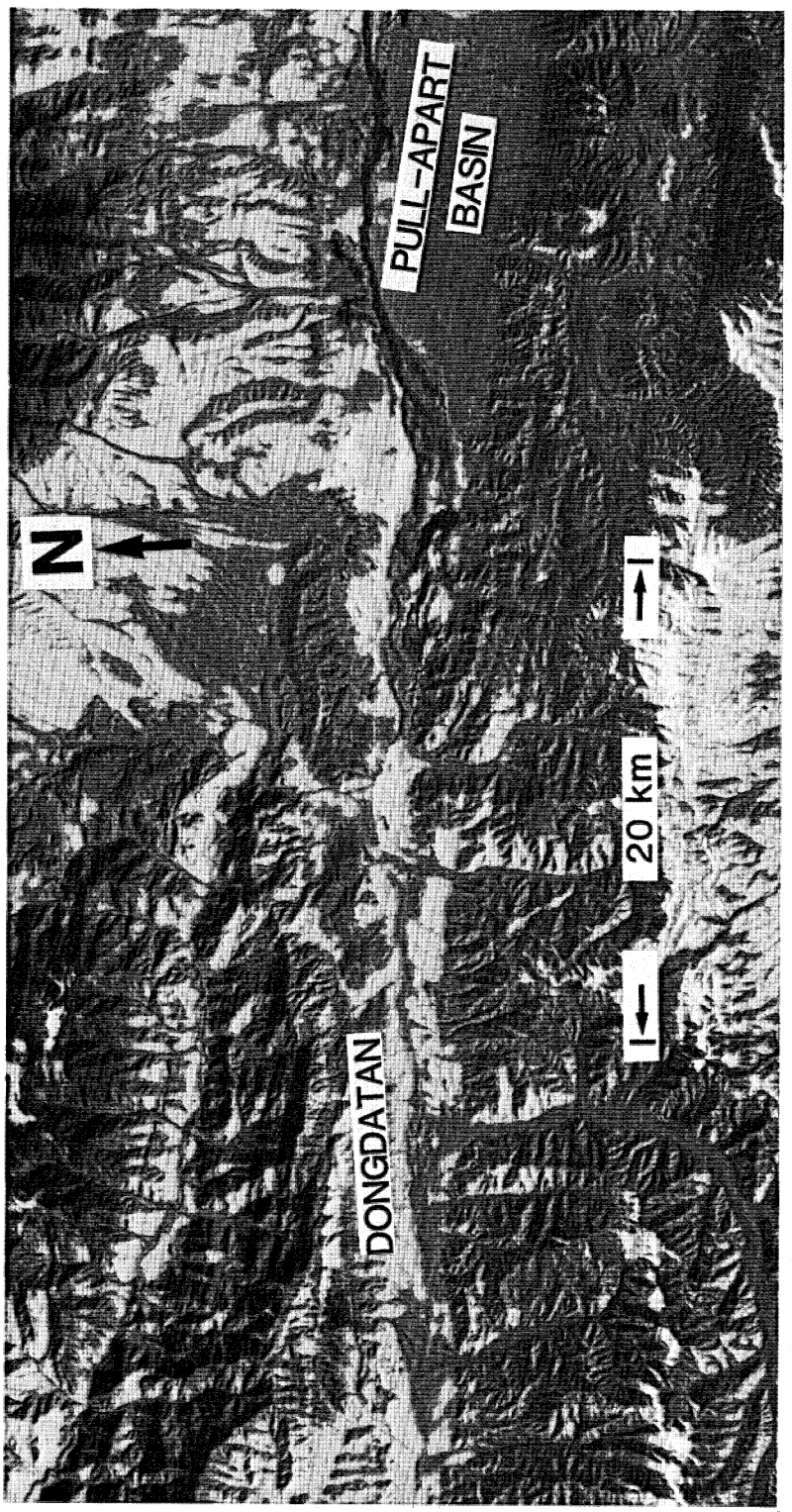

FIGURE 31. Large format camera photograph of the Dongdatan and the pull-apart basin to the east. Although the recent trace lies within the valley, segments of it have a clear topographic expression.

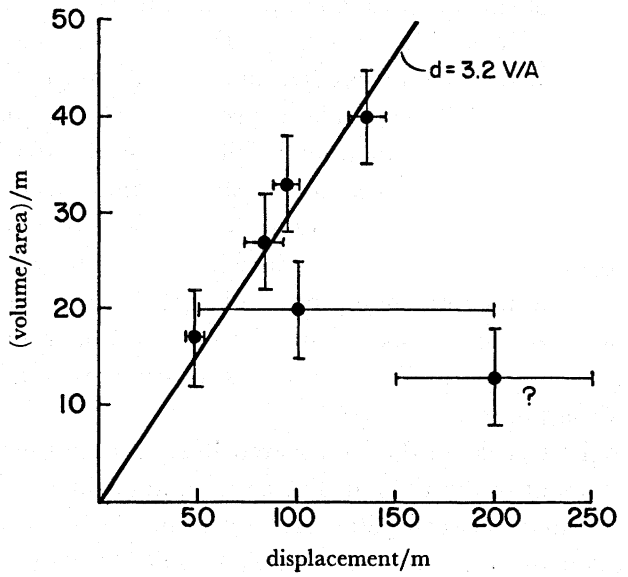

FIGURE 17. Plot of the average thickness of material eroded from the drainage basins (the ratio of the volume of the valley to its area) vs. the measured offsets of the streams. The linear relationship implies that the average erosion rate and the average slip rate on the fault are proportional to one another. Hence, the measurement of one yields an estimate of the other.

Total offset on the Kunlun Pass fault

We constructed a geologic map of the bedrock of the Kunlun Pass area (figure 12) to show the inferred distributions of the Pleistocene sequence of moraines, gravels, and lake beds and of the Triassic arenite and phyllitic slate; the cover of the very young alluvial and solifluction deposits was omitted. This map has interpolated boundaries, but at the scale mapped (1:100,000) we judge it unlikely that their positions would be altered significantly if outcrops were more widely exposed. One boundary defined within the lower part of the Pleistocene sequence, between coarser pinkish gravel below and finer, thinner bedded grey gravel above, appears to be offset 1.7 km horizontally in a left-lateral sense by the trace of the Kunlun Pass fault (asterisks in figure 12). Because the beds dip at a gentle angle (12°–20°) and strike very obliquely to the fault, this offset is a maximum for the strike-slip displacement since the gravel was deposited. Any dip-slip component of displacement (with the south side down) would reduce the real strike-slip offset. It may not be a coincidence that the contact between the lower gravel and the lake bed unit is also separated in a left-lateral sense about 3 km, but the topography in the area of the offset lake beds north of the fault implies that erosion has contributed significantly to the apparent offset in this case.

We observed another fault strand in the field a short distance south of the main fault and within the Pleistocene sequence (see figure 11), but we judge this to be a minor feature, based on its visible effects in outcrop, on its short, intermittent trace on the ground, and on the insignificance of its geomorphological expression on the satellite image compared with the main strand of the Kunlun Pass fault.

The small total strike-slip offset that we deduce contrasts strongly with the prominent geomorphological expression of the Kunlun Pass fault, at least east of the main Lhasa–Golmud highway, and with the non-trivial Holocene offset rate for this fault deduced from stream offsets.

Two features of the geomorphological expression of this fault, however, are perhaps consistent with limited total offset. First, it is difficult to trace the fault west of the Lhasa–Golmud highway, either on the ground or on Landsat MSS images and shuttle large-format camera photos, and even subtle (and somewhat debatable) expressions vanish completely 4 km west of the road. Second, when the prominent fault trace is followed on the space-based imagery to about 100 km east of where the highway crosses it, in a short distance its trend turns from 100° (along the prominent portion) to about 130° (figures 5, 9, and 10), but southeastward the topographic contrast across the fault is abruptly reduced. If the fault had extensive strike-slip displacement, this portion trending 130° should have a larger overthrust component than the portion trending 100°, and there should consequently be a major topographic expression of this thrust slip. The absence of such topographic expression is consistent with the Kunlun Pass fault having a small total strike-slip offset.

The elevation of the highest peaks in the ice-covered Burhan Budai mountains, just to the north of the prominent segment of the Kunlun Pass fault, and of the ground surface south of the fault are about 6100 m and between 4800–5100 m, respectively. If this relief developed entirely by a thrust component across the Kunlun Pass fault, then the vertical and lateral displacements on this fault would be comparable. The lack of topographic contrast across the fault, however, where the thrust component should be even larger (more than 100 km east of the highway), suggests that the relief has not developed as a result of oblique thrust and strike-slip faulting on the Kunlun Pass fault. Nevertheless, it remains the case that the Kunlun Pass fault is most prominent where the high relief occurs adjacent to it. Both to the west (where we observed it) and to the east (seen only from satellite images), the fault either disappears or is much subdued in expression where the topographic contrast lessens or vanishes.

Late Holocene faulting on the Xidatan–Tuosuohu–Maqu (Kunlun) fault

At many localities within the Xidatan and Dongdatan, we saw evidence of very recent, large-scale deformation along the most recent trace of the Xidatan–Tuosuohu–Maqu fault. This deformation includes tension gashes and mole tracks (or pressure ridges: see Richter 1958, p. 179–180 for a general description) oriented obliquely to the overall east–west trend of the fault, and offset fans, terraces, and stream channels. Many tension gashes were as deep as 1 m (in some cases 2 m) and as long as 10–20 m (in rare cases 30 m). Fresh mole tracks were of comparable dimensions. The dimensions and the freshness of these features, which are commonly associated with large earthquakes, suggest that a very large earthquake occurred on this segment of the Xidatan–Tuosuohu–Maqu (Kunlun) fault within the last few hundred years. The heights of some of the mole tracks, which must have formed by slip during several earthquakes, are more than 3 metres. In one area where recent incision by young, now dry streams had exposed cross sections through mole tracks, folds and thrust faults in very young alluvial sand and gravel were exposed. Linear ridges, with mole tracks and tension gashes crossing them, defined a zone of recent disturbance 10 to 30 m in width, and the heights of the ridges allowed this recent strand of the fault to be seen very clearly between alluvial fans where streams were flowing.

The large dimensions of the tension gashes and mole tracks made it difficult to measure reliably offsets smaller than about 10 metres. Offsets of streams and terraces of 10 to 20 m and more, however, are clear in may places. In all cases they attest to left-lateral slip. In general stream gullies shallower than about 0.5 m are not offset, but those deeper than 1 m are offset

10 m or more. In a couple of places multiple offsets could be inferred, and at one in particular, 3 or 4 repeated offsets of 10–15 m each can be inferred. Thus we conclude that movement has occurred by large amounts of slip during earthquakes.

We note that the fault zone is the locus of numerous cold springs, as are major faults throughout the world.

Below we describe and illustrate the deformation observed at individual localities. We hope that these descriptions will provide guidance for future workers on where to pursue further study of recent seismicity and deformation. We present these descriptions also in lieu of numerous, more objective large-scale contour maps. We constructed crude contour maps at two localities using a sightlevel, a compass, and a tape measure, or by pacing distances. We were not equipped with a plane-table and alidade, and we lacked the time to make additional contour maps. Using figure 13, we begin our discussion with features at the western end of the Xidatan.

Xidatan. Although the Xidatan–Tuosuohu–Maqu fault is clear on the satellite photos of the western end of the Xidatan and west of it (figures 5 and 7), and although the fault zone can be seen clearly on the ground in this area, we saw no evidence of recent slip or disruption near the western end of the Xidatan. At the westernmost locality where we did see disruption (A in figure 13), the disruption was among the least impressive of the localities that we visited. At that locality we saw a beheaded fan, low mole tracks (height $\approx$ 100s of mm) trending 130°, and shallow tension gashes trending 050°–055°. Young stream channels, however, complicate the topography.

In the 4 km east of this locality, evidence for recent deformation is not very convincing, but we did not have time to examine the area thoroughly. On the west bank of the main north–south valley and tributary to the Xidatan (B in figure 13), where the Lhasa–Golmud highway passes, fresh tension gashes and mole tracks are present.

One of us (P.M.) walked along nearly all of the segment up to 25 km east of this locality, and evidence for disruption was plentiful and clear. Approximately 1.5 km east of the valley (C in figure 13), the fault is marked by a low shutter (or pressure) ridge with mole tracks on it oriented 125°. The east side of an alluvial fan appears to be offset 10 to 30 m, but the possibility of a small vertical component of slip makes it difficult to define this value more precisely. The shutter ridge blocks a dry sag pond with dimensions of about 7 m × 10 m, and 2 m deeper than the crest of the ridge. Tension gashes 15 m in length and oriented 045° are clear. The fault zone is evident for 3 km, and no major streams or fans cross it. A shutter ridge with a height of a few metres is cut by tension gashes 100s of mm deep, 10–20 m long and oriented 045° (D in figure 13), and another small dry sag pond is clear south of the ridge (figure 19). At the east end of this zone (E in figure 13), the shutter ridge blocks, but is not dissected by, a young stream. The overall trend of the active fault is 090° ($\pm 2°$).

An actively eroding and redepositing fan without vegetation separates this segment from another farther east where the average trend of the recent scarp is 084°. The zone is marked by a prominent shutter ridge, 5 m in height, and is cut by numerous tension gashes 0.5 to 2 m deep, 5–15 m in length and trending 040°–050° (F in figure 13). One dry stream valley is offset 25–30 m left-laterally. Rounded cobbles north of the recent fault trace and now lying 11 ± 1 m west of the present main channel may imply a recent 11 ± 1 m left-lateral offset of this channel.

East of this area, deposition and erosion on large fans apparently has obliterated any recent

scarp for 2 km. Farther east a low (height < 0.4 m) south-facing, eroded scarp marks the recent trace (G in figure 13). Springs are also present. A short, north-facing scarp trends 110°, very differently oriented from the typical trend of 085°–090° (H in figure 13); probably a significant thrust component is present there.

At the west end of a high (≈ 40 m) east–west trending hill, a stream valley approximately 3 m deep is offset 15±5 m (I in figure 13). Farther east there is a sag pond on the south side of the hill. East of the hill, are clear, very large tension gashes with trends of 068°, 068°, 076°, 068°, 055°, and 068°, 0.5–2.0 m deep, 3 to 10 m wide, and up to 30 m long (J in figure 13; figures 20 and 21). An old stream terrace 0.3 m above and west of a younger stream bed has been offset left-laterally 34±5 m. The overall trend of this segment of the fault is 085°.

East of a wide stream channel (visible in figure 20), the fault zone is marked clearly by tension gashes trending 056°, mole tracks trending 145° and 155°, and a spring (K in figure 13). Farther east, the west side of an alluvial fan is offset left-laterally approximately 100 m, and the fault zone is defined by a shutter ridge 1–3 m high (L in figure 13; figure 22). Deposition and erosion are in the process of modifying the east side of the fan (the eastern side of the area shown in the contour map in figure 22). No evidence of recent faulting was seen in the gravel exposed in sections in the banks of channels.

Approximately 2 km farther east, the fault zone is again marked by numerous large tension gashes 1.5–2 m deep and trending 068° (M in figure 13). Two old terraces on the west side of an active stream have been offset 68±5 m and 75±7 m. East of another active stream, more large tension gashes, 0.5 to 1.5 m deep, trend 060° across a broad shutter ridge (width ≈ 40 m) (N in Figure 13). The west bank of a north-flowing, now dry, stream bed has been offset 15±5 m. The eastern end of this segment of the fault zone, in turn, is defined by a high shutter ridge (height ≈ 20 m) with *en echelon* hills and troughs suggestive of both tension gashes (045°) and mole tracks (120°) crossing it (O in figure 13). Prominent breaks in slope on the north side of the ridge may result from a component of thrust or reverse faulting on south-dipping faults.

We did not examine much of the 4 km east of this shutter ridge, but farther east the fault zone is again very clear. Another shutter ridge trending 080°, with relief of 2–2.5 m seems to be cut by both tension cracks and mole tracks (P in figure 13). Both dry sag ponds and springs are present on the south side of the fault trace. Farther east, on the west side of a very large fan, a high (≈ 5 m), south-facing scarp trends 085° for a distance of more than 1 km (Q in figure 13). Small hills can be seen several km farther to the east (R in figure 13) and probably mark an eastward continuation, in the direction 090°, of the active trace.

Dongdatan. We were unable to examine the 50 km of the Xidatan and Dongdatan to the east of this large scarp, but we did examine the active trace along 25 km of the Dongdatan. Springs emanate from an area near a prominent low scarp at the west end of the area studied (S in figure 23). To the east erosion and deposition along active streams and fans has obliterated this low scarp (height ≈ 1 m), but it can be seen again several km farther east (T in figure 23). Its trend is 086±2°. Low mole tracks (height ≈ 0.5 m) with dimensions of 3–4 m by 2–3 m trend northwest–southeast in the eastern part of this segment. Farther east, erosion and deposition again has obliterated any young trace.

A continuous zone of recent disruption is clear where the fault crosses a hilly area in which major streams are absent (U in figure 23). Large tension gashes 2 m deep, 20–40 m long and trending 070° are very prominent. Sag ponds, both dry and wet, are present on the north or south sides of the trace, depending upon the slope of the hilly topography.

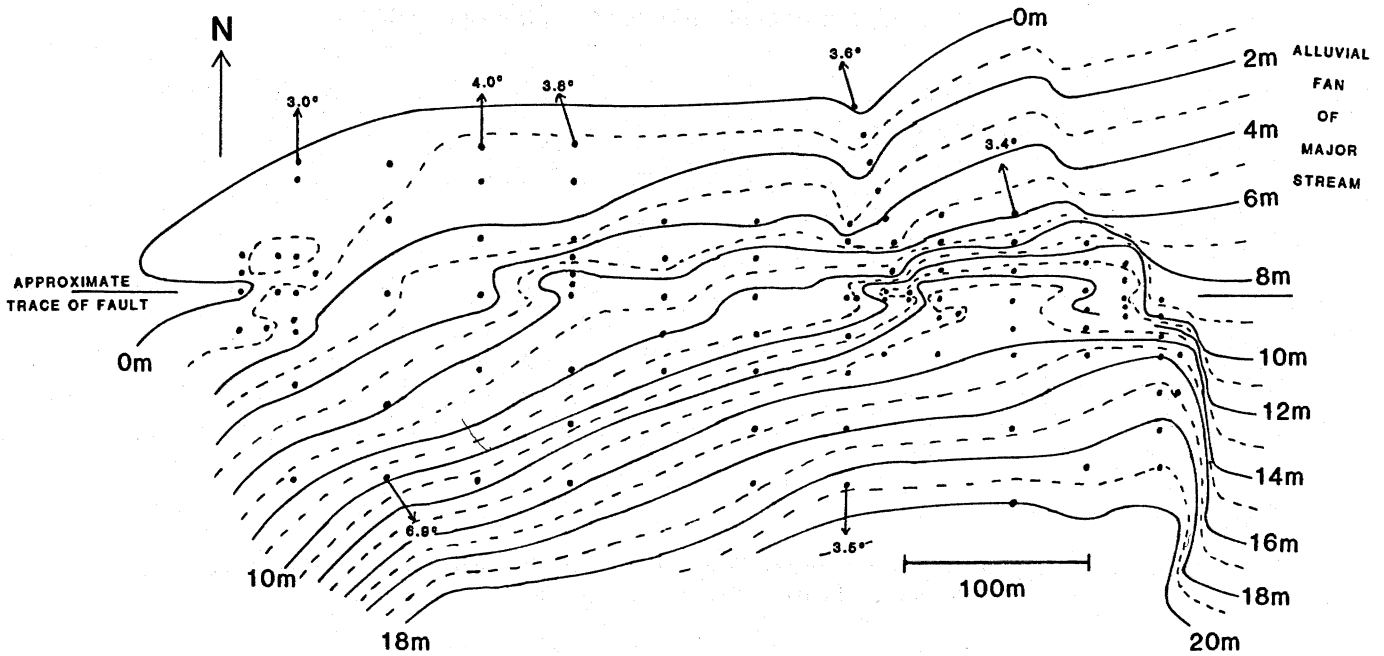

FIGURE 22. Contour map of an offset alluvial fan at locality L in figure 13. This map was made by using a tape measure or by pacing to determine distances between points, shown as dots, and a compass to determine their relative positions. Elevations were determined using a sightlevel to measure angles relative to the horizontal. Arrows give the average slopes of the surface, where it is smooth, in the directions defined by the arrows. Uncertainties in differences in elevations over distances of 100 m are about 1 m. Note the clear shutter ridge along the fault and the apparent left-lateral offset of the fan of about 100 m. At the eastern edge of the map a braided stream is actively eroding the fan and has obliterated evidence of faulting.

A large stream from the south crosses the hills and is incised into bedrock close to the fault in a locally antecedent relationship. North of the fault, the stream flows east parallel to it and has obliterated the surface expression of another 2 km of recent faulting. Farther east the fault zone lies south of the river valley, and a segment some 4 km long contains some of the most impressive evidence for recent faulting that we have ever seen. These include huge shutter ridges, sag ponds, deep tension gashes, cross sections of mole tracks, and offset gullies and stream beds.

At the west end of this segment, a dry stream bed is offset 10 ± 2 m (V in figure 23; figure 24). Farther east a prominent shutter ridge, 5 to 6 m in height bounds dry sag ponds on its south (figure 25) and is cut by huge tension gashes more than 2–3 m deep, 10–20 m in length, and with trends of about 055° (figure 26). One dry stream bed seems to have been multiply offset (W in figure 23). Two northward-flowing streams merge at the scarp, which is marked by a prominent shutter ridge (figure 27). Three or four groups of rounded cobbles on the north side of the fault appear to mark abandoned stream channels that apparently have successively been displaced westward by slip on the fault (figure 28). Spacings between them of 11 m, 11 m, 10 m, and roughly 8 m (or possibly 1 of 15 to 18 m) (figure 28) suggest that slip has occurred by discrete events of comparable magnitude and probably not by continuous fault creep.

The high shutter ridge with heights reaching 6 to 7 m continues east for 2 km (X in figure 23) and is cut by huge tension gashes, more than 3 m deep in one case and trending 030° to 060°. The fault zone is quite wide, up to 50 m, and within that zone gravels have been tilted

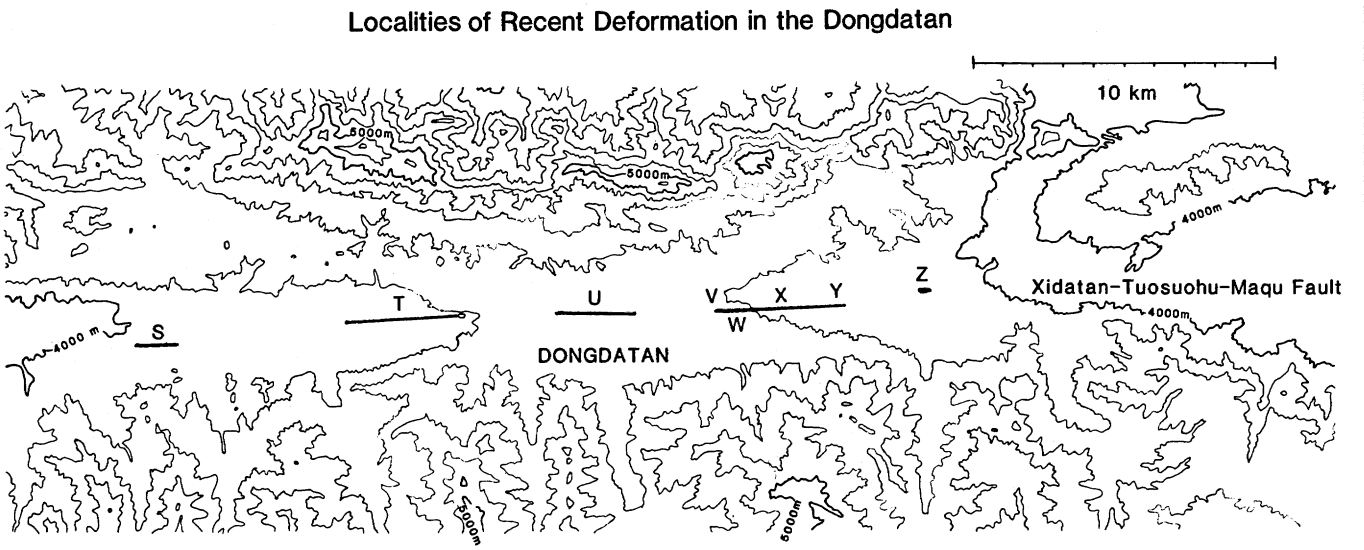

FIGURE 23. Map showing areas of recent disruption along the Xidatan–Tuosuohu–Maqu fault in the Dongdatan. Letters correspond to areas discussed in the text.

from 20°–30° to as much as 55° (Y in figure 23; figure 29). Cross sections exposed by streams through mole tracks and through the main shutter ridge reveal thrust faulting and folding within these young deposits (figure 30). These features are clearly due to localised horizontal compression.

Erosion and deposition seem to have obliterated much of the recent deformation in the 3 km farther east, but an east–west alignment of low mounds (height ≈ 0.5 m) seems to mark the fault zone on a large fan (Z in figure 23). They might be eroded mole tracks. We did not have time to examine features farther east, where the fault enters a large pull-apart basin (figure 31).

Summary of late Holocene deformation along the Xidatan–Tuosuohu–Maqu fault.

The features described above attest to recent strike-slip faulting on this fault, and they suggest that this displacement has occurred by slip during large earthquakes. The last such earthquake probably occurred within the last few hundred years.

Young disruption is clear along at least 110 km of the fault, the distance between the westernmost and the easternmost points of observation. This disruption includes large mole tracks and deep tension cracks, features commonly associated with earthquakes (Richter 1958, pp. 179–180). If all of the disruption occurred during the same event, then by comparison with other events in Asia, a maximum fault length of 110 km would imply that the magnitude of the earthquake was at least $7\frac{1}{2}$ (e.g. Molnar & Deng 1984).

Many of the tension cracks are bounded by free faces; thus they are in a youthful stage of erosion. By analogy with free faces on fault scarps, the existence of free faces implies that the tension cracks are only a few hundred years old, and possibly only 100 years old (Wallace 1977). Permafrost did not seem to be present in this area, and consequently these features probably have not been maintained for unusually long times by frozen ground. They probably are not associated with the 19 April 1963 earthquake with $M = 7.0$, which occurred 210 km east of our westernmost observation. The large scale of the deformation and the required fault

length of 200 km are both greater than what are likely for an event with a magnitude of only 7.0. No other earthquake with a magnitude greater than 7 is listed by Gutenberg & Richter (1954), Duda (1965), or Geller & Kanamori (1977) for this region in this century. Thus, the earthquake responsible for the tension gashes and mole tracks probably occurred before 1900, but almost certainly since 1500 to 1700 A.D.

The dimensions of the tension cracks and mole tracks are unusually large–larger than those of the 1920 Haiyuan earthquake (M = 8.7), for which the average displacement was 8 m and for which the displacement in places reached 10–12 m (Deng *et al.* 1984, 1986; Zhang *et al.* 1987). The observations of displaced stream gullies of 10 to 15 m at various localities along the Xidatan–Tuosuohu–Maqu fault are sufficiently numerous to suggest that offset of this amount occurred during the same earthquake responsible for the tension cracks and mole tracks, but the difficulties in measuring smaller offsets allow for this inference to be false. The groups of cobbles that seem to indicate abandoned channels of a successively displaced stream channel in the Dongdatan (figure 28), however, also concur with repeated offsets of 10–15 m. The observations from this one locality also are not, by themselves, enough to prove that slip has occurred in jumps of 10 to 15 m during large earthquakes, but we think that this is the most sensible interpretation of the distribution of cobbles shown in figure 28.

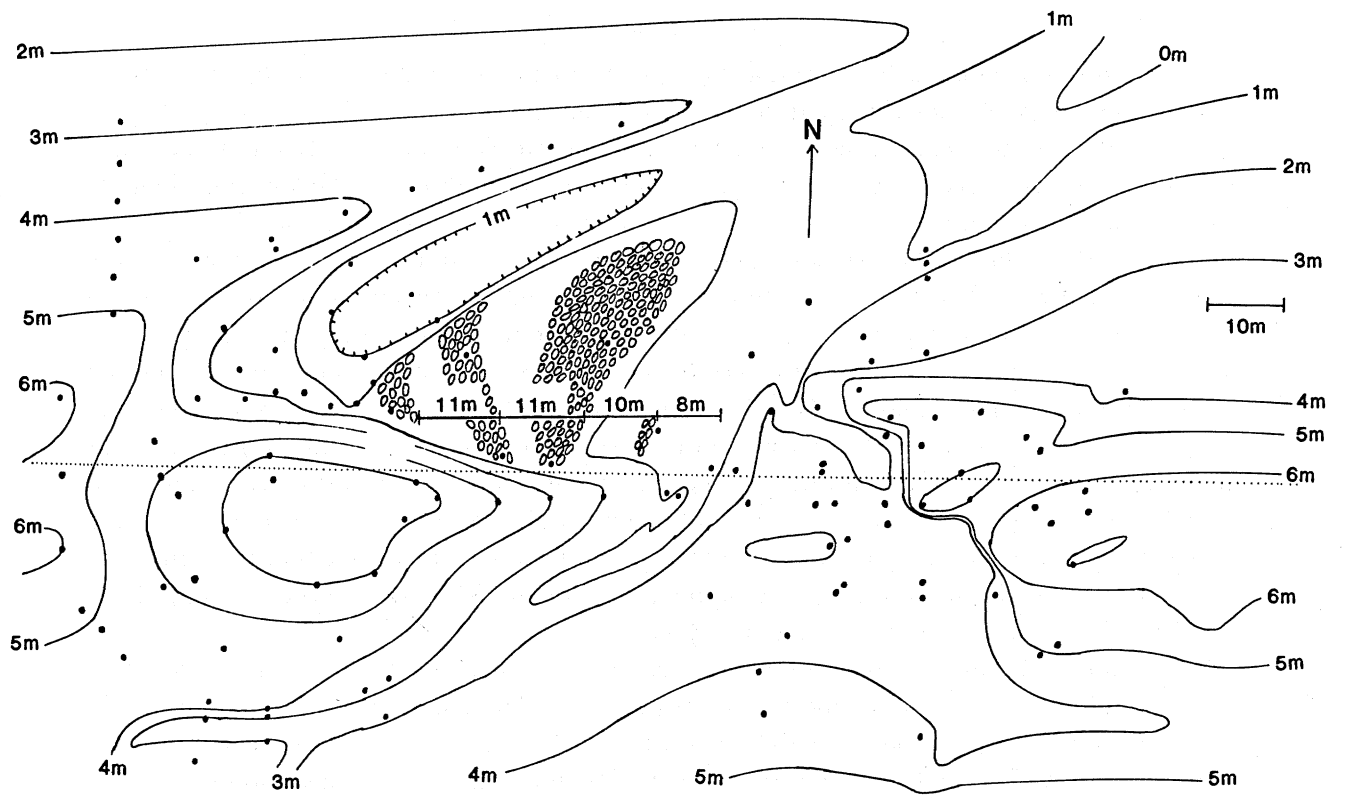

FIGURE 28. Contour map of the area shown in figure 27. Groups of cobbles are shown in areas separated from one another by 11 m, 11 m, and 10 m. We interpret these as having been deposited by the ancestral stream of that shown crossing the fault and presently about 8 m east of the easternmost, small group of cobbles. Thus these observations seem to indicate multiple offsets of the stream. Probably at an earlier stage the stream passed through the area including the closed contour northwest of the groups of cobbles. Note also the subtle northeast trend of topography on the prominent easterly trending shutter ridge, which is apparent in the shape of the 6 m contour; this northeast trend reflects the existence of tension gashes obliquely crossing the shutter ridge.

We have no evidence constraining the recurrence intervals of such large earthquakes. If the slip rate is 10 or 20 mm/a, as discussed above, and if large events can be associated with 10 or 15 m of slip, then recurrence intervals are likely to be between 500 and 1500 years. The steepness of erosional escarpments offset 20 to 40 m, presumably by 2 or more earthquakes, certainly allows them to be only a few thousand years old, but we lack any useful quantitative observations to constrain the recurrence interval.

Unfortuantely we found no clear Holocene or post-glacial features, such as moraines, that were offset and that could be used to estimate a Holocene average slip rate. The offsets of small streams and of fans, of as much as 100 m in one case, could have occurred during late Holocene time, or if the average rate of slip were only 10 mm/a, they could represent slip during the entire Holocene. Unfortunately, we could not date them.

Thus, the recent disruption along the Xidatan–Tuosuohu–Maqu fault attests to its recent activity. The types of features – tension gashes and mole tracks – imply the occurrence of a recent earthquake. The dimensions of these features and the amounts of offsets of gullies and dry stream valleys imply that that earthquake was very large. Finally we suspect that slip has occurred several times in the last few thousand years by displacement of 10 to 15 m during earthquakes.

Conclusions

Our most significant conclusion is that the rate of slip on the Kunlun strike-slip fault system is more than 10 mm/a for the Quaternary period, and possibly more than 20 mm/a for the most recent 10 ka to 20 ka. A moraine, presumably of late Pliocene or early Quaternary age and containing very distinctive blocks of pyroxenite, has been displaced 30 km from the only known outcrop of pyroxenite in the area, an outcrop that lies very near to the Xidatan–Tuosuohu–Maqu fault, the principal active fault in the Kunlun system. If the age of the moraine is 2.4 Ma, then the rate of slip is about 13 mm/a, with minimum and maximum possible values 10 and 20 mm/a. Stream valleys crossing a second fault in the Kunlun fault system, the Kunlun Pass fault, are displaced 50 to 150 m. Several observations suggest that the incision of these valleys began in the latest Pleistocene or Holocene epochs, and if so then the average rate of slip on this fault is also about 10 mm/a (between 5 and 20 mm/a). Detailed mapping of gravel layers beneath the lake beds revealed a small offset of this gravel unit: less than 1.7 km. Thus we suspect that the Kunlun Pass fault may not have been active for the whole of the Quaternary period. Accordingly, it would be unwise to assume that the sum of the Holocene rate for this fault and the Quaternary rate for the Xidatan–Tuosuohu–Maqu fault is applicable to the whole of the Quaternary period.

We found abundant evidence for very recent disruption along the Xidatan–Tuosuohu–Maqu fault in both the Xidatan and the Dongdatan. Very large tension gashes and mole tracks attest to surface deformation, probably associated with a major earthquake, in the last few hundred years. Offsets of several features of about 10 m imply that slip of that amount occurred during such an earthquake, and the distribution of stream cobbles deposited in apparently successively offset stream channels, suggest multiple offsets of this amount. We conclude that the Xidatan–Tuosuohu–Maqu fault is still very active, and that slip on it probably occurs abruptly in rare large earthquakes. Moreover, the apparent recent initiation of slip on the Kunlun Pass fault probably should not be associated with any decline in the rate of slip on the Xidatan–Tuosuohu–Maqu fault.

A correlation of the truncation of a well-defined phyllonitic unit, mapped in the Kunlun Pass area, with a light-coloured unit, seen on the Landsat imagery of the area north of the Xidatan–Tuosuohu–Maqu fault and 75 km west of the Kunlun Pass, suggests a minimum total offset of 75 km for that fault.

In addition recent normal faulting was observed in a northerly-trending half-graben near Wenquan, and recent deformation of thrust and probably strike-slip sense was observed in the northeasterly-trending valley containing the town of Amdo and at the southern margin of the Erdaogou range (figure 1). Such observations of reverse or thrust faulting are unusual *within* the high plateau, where the active tectonics are characterized by normal and strike-slip faulting. Nevertheless, from the linearity of the scarps, the fault plane solution of nearby earthquakes, and the orientations of a few slickensides, we infer that the left-lateral strike-slip displacements are comparable with the vertical components, and that these localized examples of thrust faulting probably are not reliable indicators of the regional tectonic strain field.

The prevalence of normal faulting on northerly-trending grabens in southern Tibet (e.g. Armijo *et al.* 1986), and the conjugate strike-slip faulting, with left-lateral slip on northwesterly-striking planes and right-lateral slip on northeasterly-striking planes, reflect an east–west extension of the plateau and an eastward extrusion of the crust within Tibet (e.g. Molnar & Tapponnier 1975, 1978). Left-lateral slip on the Kunlun strike-slip fault system of more than 10 mm/a, and possibly at 20 mm/a in the last 10 ka shows that the area south of the Kunlun is being rapidly displaced eastward with respect to the area farther north. This eastward displacement is probably a consequence of the continuing penetration of India into the rest of Eurasia (e.g. Molnar & Tapponnier 1975; Tapponnier & Molnar 1977). The high elevation and thick crust of the Tibetan Plateau make further crustal thickening of Tibet energetically difficult, and eastward extrusion of the plateau allows India's penetration without further increase in the gravitational potential energy stored in Tibet's crust (e.g. England & Houseman 1986; Molnar & Lyon-Caen 1988; Molnar & Tapponnier 1978).

The rapid rate of slip implies a correspondingly rapid rate of extrusion, which manifests itself both by active mountain building on the eastern edge of the plateau and by the eastward expulsion of southeast China over the Pacific and Philippine sea plates. The demonstration of this rapid displacement in a direction perpendicular to the direction of convergence of the Indian and Eurasian plates is a reminder of how difficult it is, in general, to infer the direction of relative plate motion in ancient orogenic belts solely from the strain within those belts, especially in only small fragments of them.

We thank the logistic staff of Academia Sinica, in particular Ma Xuezheng and Wang Zhe, and of the Royal Society, particularly L. U. Mole, for making the Geotraverse efficient and productive, and also the driver, Chen Guozhen, whose bold driving took us to places ordinarily too far to reach. We also thank K. C. A. Burke for the loan of large format camera images and for the use of the image processing facilities of the Lunar and Planetary Institute. He, J. A. Jackson, and K. Sieh made helpful suggestions for the improvement of the manuscript, and S. A. Schumm offered some guidance with erosion rates. This research was supported in part by the National Science Foundation through grant EAR-8417640 and by NASA through grant NAG-G5-524.

Chang Chengfa, J. F. Dewey, A. Gansser and J. A. Pearce participated in the field work and offered helpful suggestions. John Dewey, in particular, pointed out the incised meanders in the Erdaogou region and their implications for recent activity there.

References

Armijo, R., Tapponnier, P., Mercier, J. L. & Han Tonglin 1986 Quaternary extension in southern Tibet: Field observations and tectonic implications. *J. geophys. Res.* **91**, 13,803–13,872.

Armijo, R., Tapponnier, R. & Han Tonglin (in press) Late Cenozoic right-lateral strike-slip faulting across southern Tibet. *J. geophys. Res.* **93**.

Brune, G. 1948 Rates of sediment production in midwestern United States. *Soil Conservation Service Tech. Pub. 65*, 40 pp.

Burchfiel, B. C., Zhang Peizhen, Wang Yipeng, Zhang Weiqi, Jiao Decheng, Song Fangmin, Deng Qidong, Molnar, P., & Royden L. (in press) Geology of the Haiyuan Fault Zone, Ningxia-Hui Autonomous Region, China and its Relation to the Evolution of the Northeastern Margin of the Tibetan Plateau. *Bull. geol. Soc. Am.*

Burke, K. C. A. & Lucas, L. (in press) Lumpola Basin: Thrusting on the Tibetan Plateau within the last 5 Ma. In *Tectonic Evolution of the Tethyan Regions* (ed. A. M. C. Sengör). Nato Advanced Study Institute. Dordrecht: Reidel.

Burke, K. C. A., Dewey, J. F. & Kidd W. S. F. 1974 The Tibetan Plateau, Its significance for tectonics and petrology. *Geol. Soc. Amer. Abstr. Programs* **6**, 1027–1028.

Chang Chengfa, Chen Nansheng, Coward, M. P., Deng Wanming, Dewey, J. F., Gansser, A., Harris, N. B. W., Jin Changwei, Kidd, W. S. F., Leeder, M. R., Li Huan, Lin Jinlu, Liu Changjie, Mei Houjun, Molnar, P., Pan Yun, Pan Yusheng, Pearce, J. A., Shackleton, R. M., Smith, A. B., Sun Yiyin, Ward, M., Watts, D., Xu Juntao, Xu Ronghua, Yin Jixiang & Zhang Yuquan 1986 Preliminary conclusions of the Royal Society and Academia Sinica 1985 Geotraverse of Tibet, *Nature, Lond.* **323**, 501–507.

Cui Zhengyuan & Yang Bin 1979 On the Tuosuohu–Maqu active fault zone (in Chinese). *Northwest. seismol. Jl.* **1**(2), 57–61.

Deng Qidong, Song Fangmin, Zhu Shilong, Li Mengluan, Wang Tielin, Zhang Weiqi, Burchfiel, B. C., Molnar, P. & Zhang Peizhen 1984 Active faulting and tectonics of the southern Ningxia-Hui Autonomous Region, *J. geophys. Res.* **89**, 4427–4445.

Deng Qidong, Chen Shefa, Song Fangmin, Zhu Shilong, Wang Yipeng, Zhang Weiqi, Jiao Decheng, Burchfiel, B. C., Molnar, P., Royden, L. & Zhang Peizhen 1986 Variations in the geometry and amount of slip on the Haiyuan fault zone and the surface rupture of the 1920 Haiyuan earthquake. *Maurice Ewing Series* **6**, Amer. Geophys. Un., Washington, D.C., 160–182.

Duda, S. J. 1965 Secular seismic energy release in the circum-Pacific belt. *Tectonophysics* **2**, 409–452.

England, P. C. & Houseman, G. A. 1986 Finite strain calculations of continental deformation; 2. Comparison with the India–Asia collision. *J. geophys. Res.* **91**, 3664–3676.

Geller, R. J. & Kanamori H. 1977 Magnitude of great shallow earthquakes from 1904 to 1952. *Bull. seismol. Soc. Amer.* **67**, 587–598.

Gutenberg, B. & Richter, C. F. 1954 *The Seismicity of the Earth.* 310 pp. New York: Hafner.

Hennig, A. 1915 *Zur Petrographie und Geologie von Sudwestibet, Southern Tibet*, vol. V. Stockholm: Kung. Boktryekeriet. P. A. Norstedt.

Holmes, A. 1965 *Principles of Physical Geology.* London: Thomas Nelson & Sons Ltd. Chapter XXI.

Kidd, W. S. F. 1975 Widespread late Neogene and Quaternary alkaline volcanism on the Tibetan Plateau. (abstract). *EOS. Trans. Amer. geophys. Un.* **56**, 453.

Langbein, W. B. & Schumm, S. A. 1958 Yield of sediment in relation to mean annual precipitation. *Trans. Amer. geophys. Un.* **39**, 1076–1084.

Lee, K. Y. 1984 Tertiary system and its petroleum potential in the Lunpola Basin, Xizang (Tibet). *Open-File Report 84–420.* U.S. Geologic Survey.

Li Longhai & Jia Yunhong 1981 Characteristics of the deformation band of the 1937 Tuosuohu earthquake ($M = 7.5$) in Qinghai (in Chinese). *Northwest. seismol. Jl.* **3**(3), 61–65.

Littledale, St. G. R. 1896 A journey across Tibet, from north to south, and west to Ladak. *Geogr. Jl.* **7**, 453–483.

Molnar, P. & Chen W.-P. 1983 Focal depths and fault plane solutions of earthquakes under the Tibetan plateau. *J. geophys. Res.* **88**, 1180–1196.

Molnar, P. & Deng Qidong 1984 Faulting associated with large earthquakes and the average rate of deformation in central and eastern Asia. *J. geophys. Res.* **89**, 6203–6227.

Molnar, P. & Lyon-Caen H. 1988 Some simple physical aspects of the structure, support, and evolutions of mountain belts. *Geol. Soc. Am. Spec. Pap.* 218, pp. 179–207.

Molnar, P. & Tapponnier P. 1975 Cenozoic tectonics of Asia: Effects of a continental collision. *Science, Wash.* **189**, 419–425.

Molnar, P. & Tapponnier P. 1978 Active tectonics of Tibet. *J. geophys. Res.* **83**, 5361–5375.

Molnar, P., Chen, W.-P., Fitch, T. J., Tapponnier, P., Warsi, W. E. K. & Wu, F. T. 1977 Structure and tectonics of the Himalaya: A brief summary of relevant geophysical observations. *Colloque Internationaux du CNRS, No. 268, Himalaya: Sciences de la Terre.* Editions du centre National de la Recherche Scientifique, Paris, 269–294.

Molnar, P., Burchfiel, B. C., Zhao Ziyun, Liang K'uangyi, Wang Shuji & Huang Minmin 1987*a* The geologic evolution of northern Tibet: Results from an expedition to Ulugh Muztagh. *Science, Wash.* **235**, 299–305.

Molnar, P., Burchfiel, B. C., Liang K'uangyi & Zhao Ziyun 1987*b* Geomorphic evidence for active faulting in the Altyn Tagh and northern Tibet and qualitative estimates of its contribution to the convergence of India and Eurasia. *Geology* **15**, 249–253.

Ni, J. & York, J. E. 1978 Late Cenozoic extensional tectonics of the Tibetan Plateau. *J. geophys Res.* **83**, 5377–5387.

Norin, E. 1946 Geological Explorations in Western Tibet. *Reports from the Scientific Expedition to the Northwestern Provinces of China under the Leadership of Dr. Sven Hedin, Publ. 29, (III), Geology 7.* Thule, Stockholm: Tryckeri Aktiebolaget.

Qian Fang, Ma Xinghua, Wu Xihao & Pu Qingyu 1982 Study of the magnetic stratigraphy of the Qiangtang and Quguo formations (in Chinese). *Contributions to the Geology of the Qinghai-Xizang (Tibet) Plateau* **4**. Beijing: Geol. Pub. House, 121–130.

Richter, C. F. 1958 *Elementary Seismology*, San Francisco: W. H. Freeman, pp. 179–180.

Rothery, D. A. & Drury S. A. 1984 The neotectonics of the Tibetan Plateau. *Tectonics* **3**, 19–26.

Schumm, S. A. 1963 *The Disparity Between Present Rates of Denudation and Orogeny. U.S. Geol. Surv. Prof. Paper 454-H.* U.S. Govt. Printing Office.

Sengör, A. M. C. & Kidd, W. S. F. 1979 Post-collisional tectonics of the Turkish-Iranian Plateau and a comparison with Tibet. *Tectonophysics* **55**, 361–376.

Shackleton, N. J., Backman, J., Zimmerman, H., Kent, D. V., Hall, M. A., Roberts, D. G., Schnitker, D., Baldauf, J. G., Desprairies, A., Homrighausen, R., Huddlestun, P., Keene, J. B., Kaltenback, A. J., Krumsiek, K. A. O., Morton, A. C., Murray, J. W. & Westberg-Smith J. 1984 Oxygen isotope calibration of the onset of ice-rafting and history of glaciation in the North Atlantic region. *Nature, Lond.* **307**, 620–623.

Tapponnier, P. & Molnar, P. 1977 Active faulting and Cenozoic tectonics of China. *J. geophys. Res.* **82**, 2905–2930.

Tapponnier, P. *et al.* 1981*a* The Tibetan side of the India Eurasia collision. *Nature, Lond.* **294**, 405–410.

Tapponnier, P., Mercier, J. L., Armijo, R., Han T. & Zhou J. 1981*b* Field evidence for active normal faulting in Tibet. *Nature, Lond.* **294**, 410–414.

Tapponnier, P., Peltzer, G., Le Dain, A. Y., Armijo, R. & Cobbold, P. 1982 Propagating extrusion tectonics in Asia: New insights from simple experiments with plasticine. *Geology* **10**, 611–616.

Tapponnier, P., Peltzer, G. & Armijo, R. 1986 On the mechanics of the collision between India and Asia. In *Collision Tectonics* (ed. M. P. Coward & A. C. Ries) Geological Society, London, pp. 115–157.

Wallace, R. E. 1977 Profiles and ages of young fault scarps, north-central Nevada. *Bull. geol. Soc. Am.* **88**, 1267–1281.

Wu Xihao, Qian Fang & Pu Qingyu 1982 Quaternary glaciogeology of the east Kunlun mountains (in Chinese). *Contributions to the Geology of the Qinghai-Xizang (Tibet) Plateau* **4**, 1–18. Beijing: Geol. Pub. House.

Zhang Weiqi, Jiao Decheng, Zhang Peizhen, Molnar, P., Burchfiel, B. C., Deng Qidong & Wang Yipeng 1987 Displacement along the Haiyuan fault associated with the great 1920 Haiyuan, China, earthquake. *Bull. seismol. Soc. Am.* **77**, 117–131.

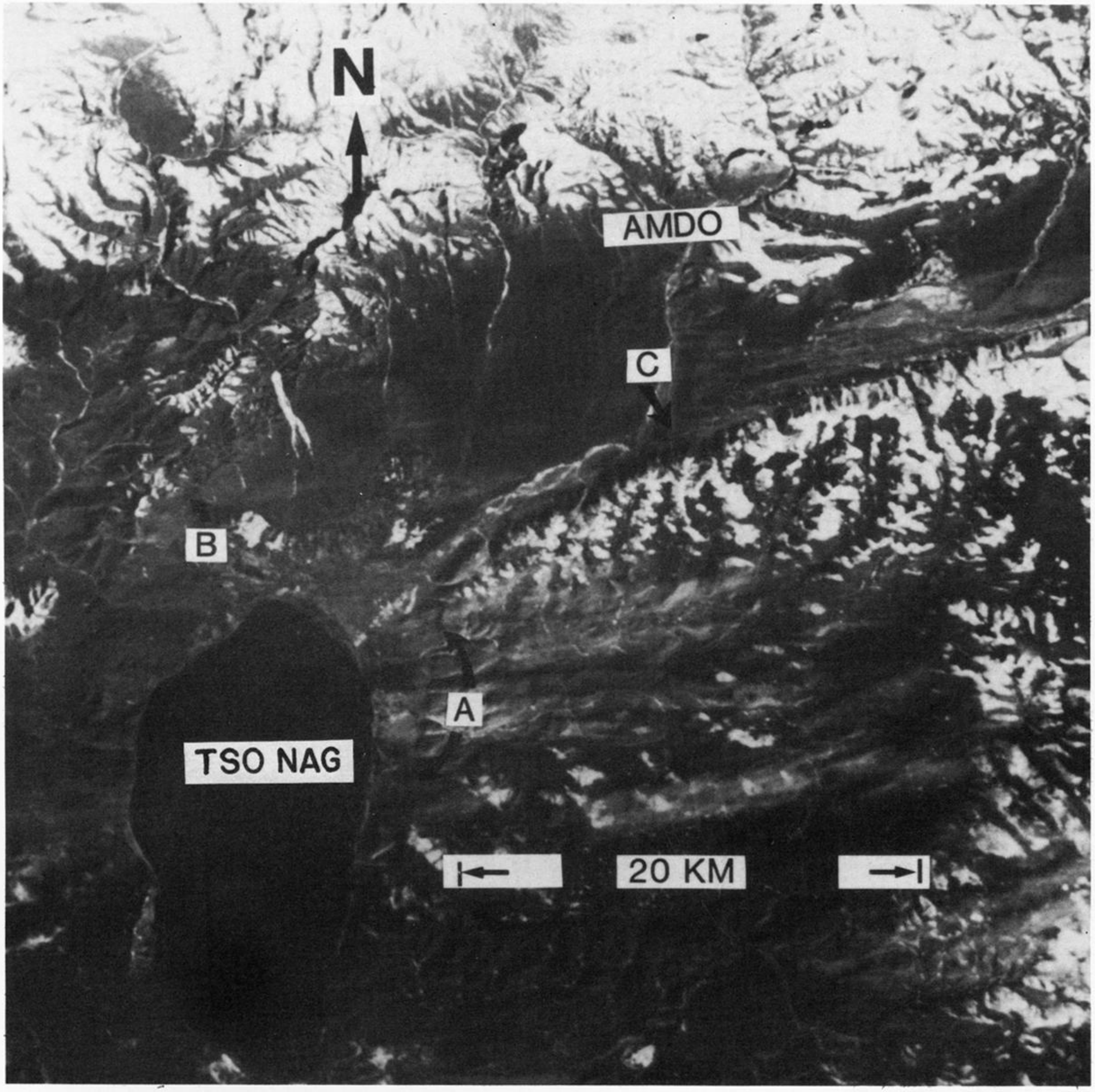

FIGURE 2. Portion of a shuttle metric camera photograph showing the area near Amdo and the lake Tso Nag (figure 1). Note the clear scarp on the east side of Tso Nag (A), which we presume to mark an active or recently active normal fault. To the northeast, the valley containing the town of Amdo is bounded by linear scarps, along which we think there is a large strike-slip component. At C, recent sand and gravel is disrupted (figure 3). At B, there is a component of thrust or reverse faulting, but the linearity of the scarp suggests that there is a significant strike-slip component.

FIGURE 3. Photograph, taken at C in figure 2, showing folded and faulted layers of sand and gravel along a zone where oblique normal and left-lateral strike-slip faulting seems to have occurred. The view is to the south.

FIGURE 4. Photograph of young scarp near hot springs on the west side of a graben (or half-graben) near Wenquan (figure 1). View is to the west-southwest.

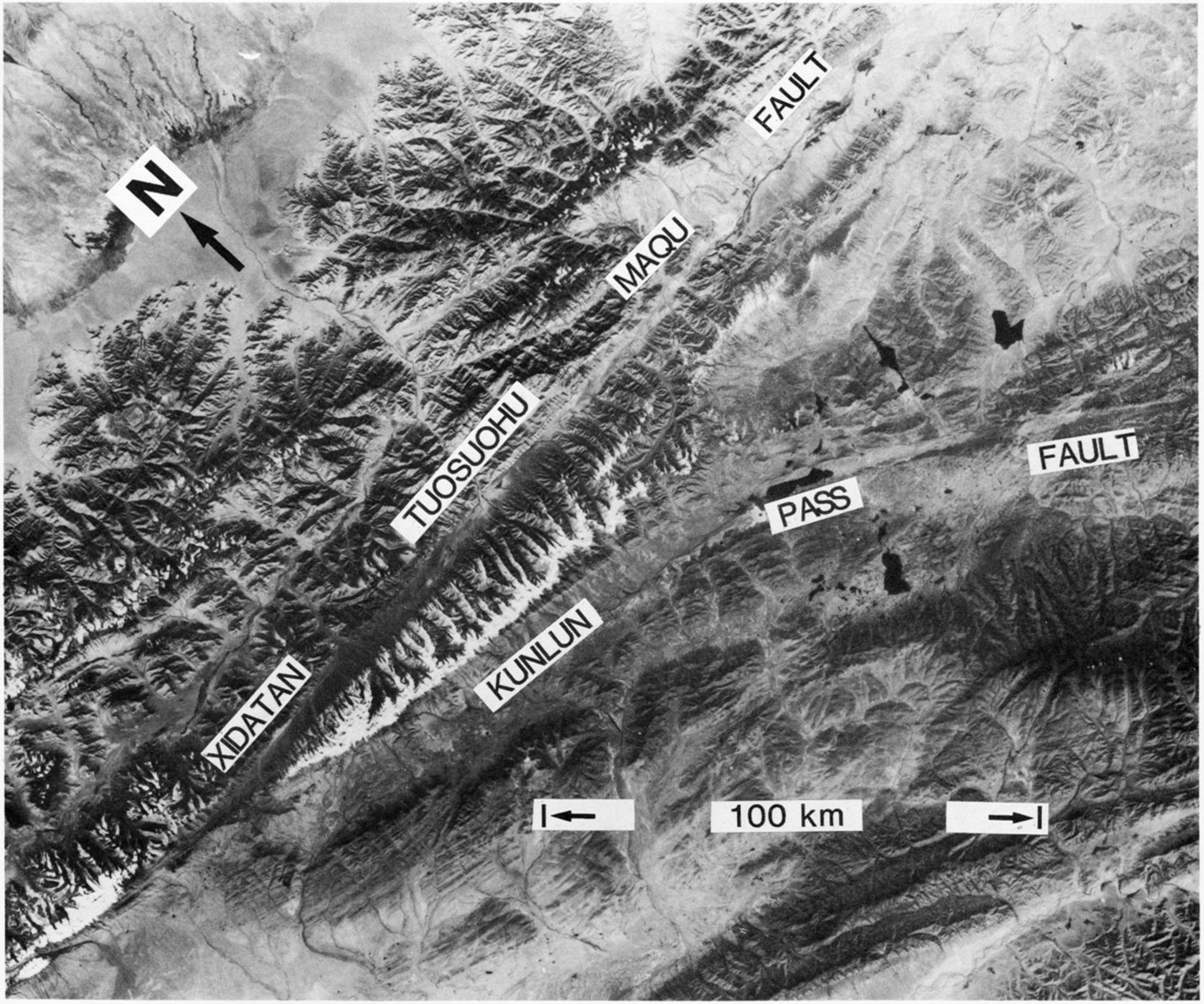

FIGURE 5. Large format camera photograph of the area including the Xidatan, Burhan Budai, and Kunlun Pass region. The Burhan Budai is the easterly-trending snow-capped range in the west-central part of the image between the Xidatan–Tuosuohu–Maqu and Kunlun Pass faults. The Xidatan–Tuosuohu–Maqu fault passes north of the Burhan Budai through the easterly-trending valleys, the Xidatan (figures 7 and 8) and Dongdatan (figures 23 and 31), and continues into a large pull-apart structure (figure 31). South of the Burhan Budai the Kunlun Pass fault is visible at the break in slope at the foot of the range (figure 14). Toward the west the Kunlun Pass fault approaches the Xidatan–Tuosuohu–Maqu fault but does not appear to intersect it (see figure 8).

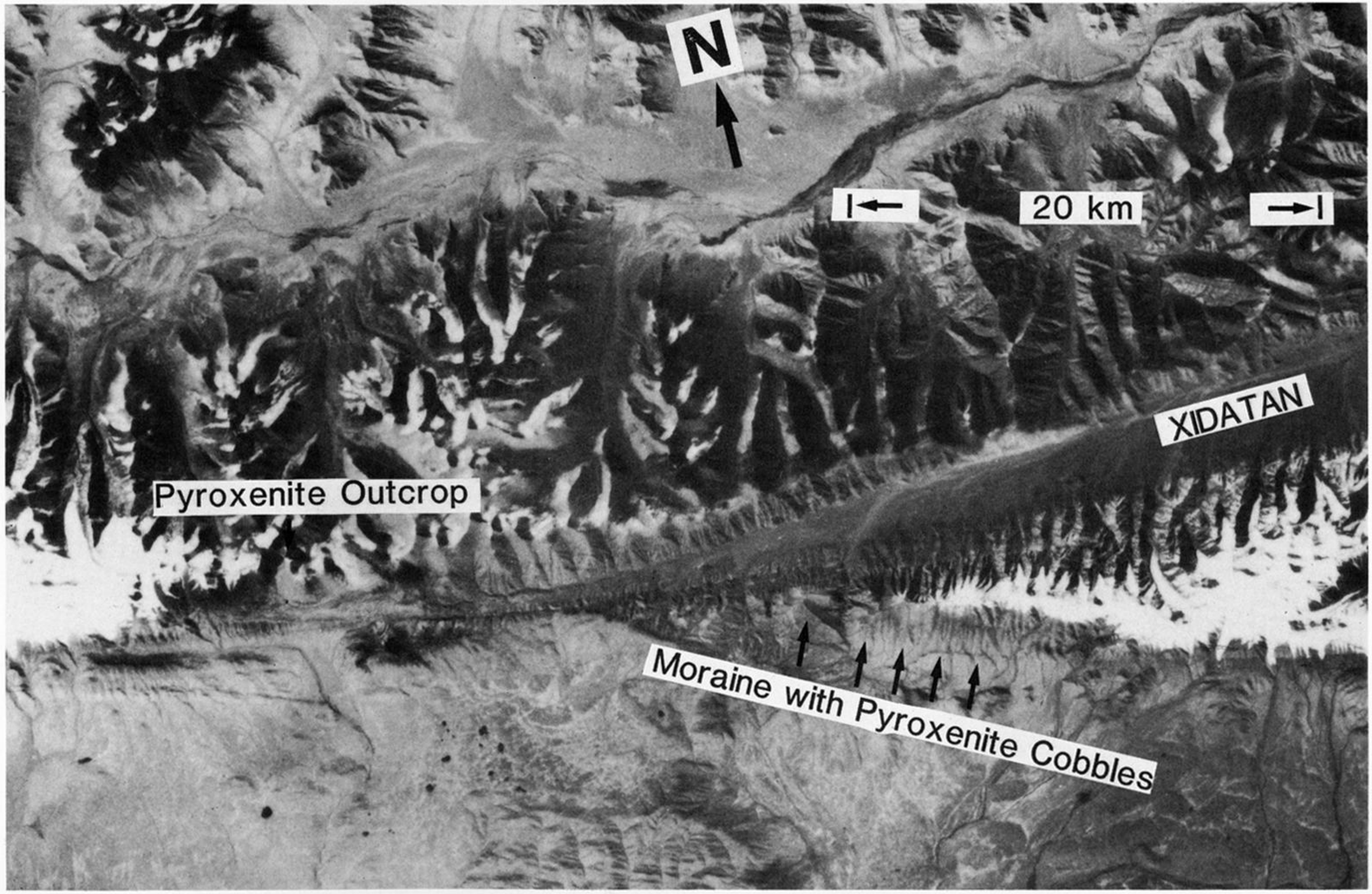

FIGURE 8. Large format camera photograph of the area where the Xidatan–Tuosuohu–Maqu and Kunlun Pass faults approach one another showing the locations of the outcrop of pyroxenite and the moraines containing pyroxenite cobbles.

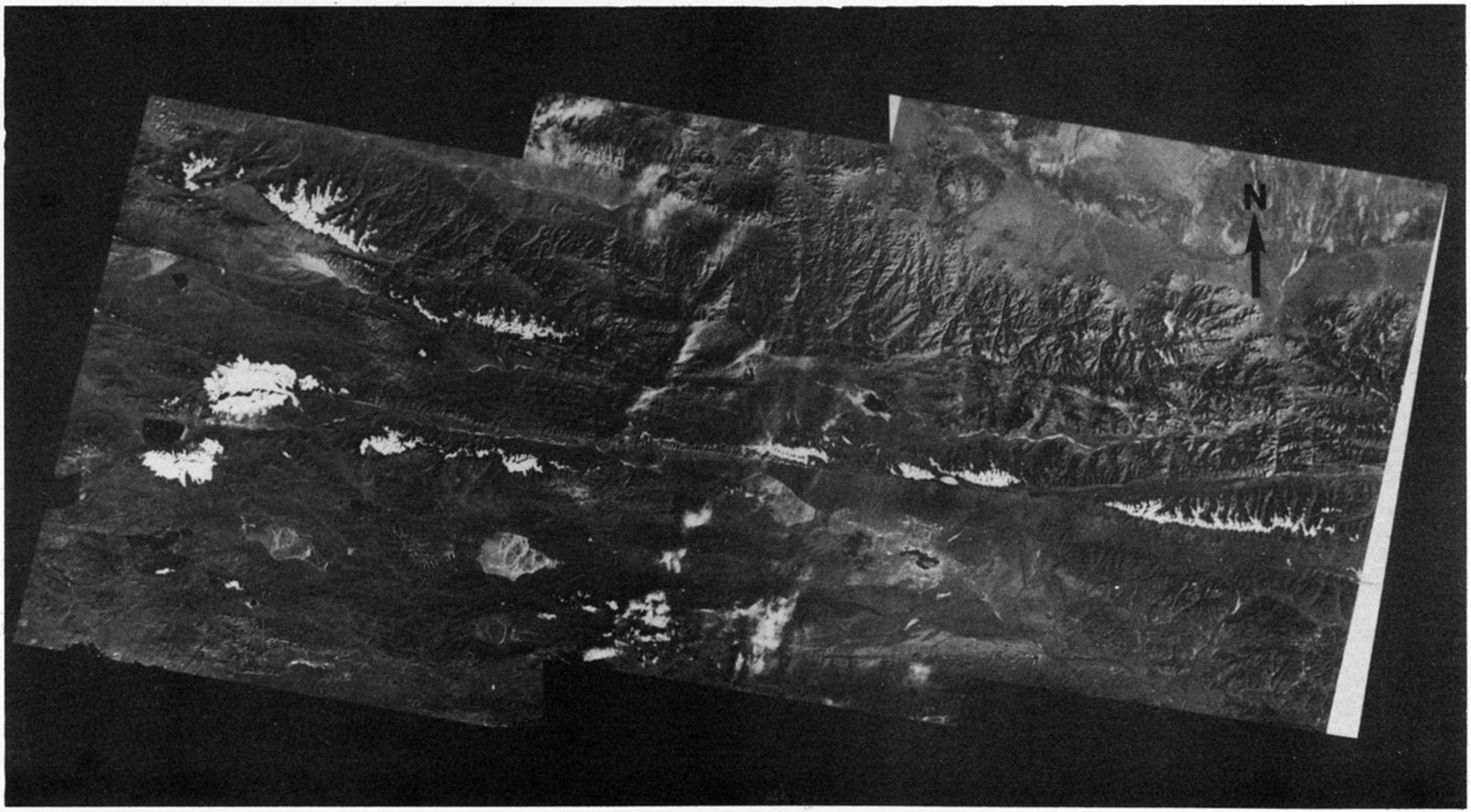

FIGURE 10. Mosaic of three Landsat images covering a portion of the western reaches of the Kunlun fault system. The main Xidatan–Tuosuohu–Maqu fault extends from about 90.5° E to 95° E on this mosaic. The traverse line crosses this fault in the Xidatan, near Kunlun Pass (see figure 9 to locate the mosaic). The minor faults and linear features identified in the area of the mosaic are indicated on figure 9. Locations of possible offset continuations of the phyllonite unit identified on these images are shown on figure 11.

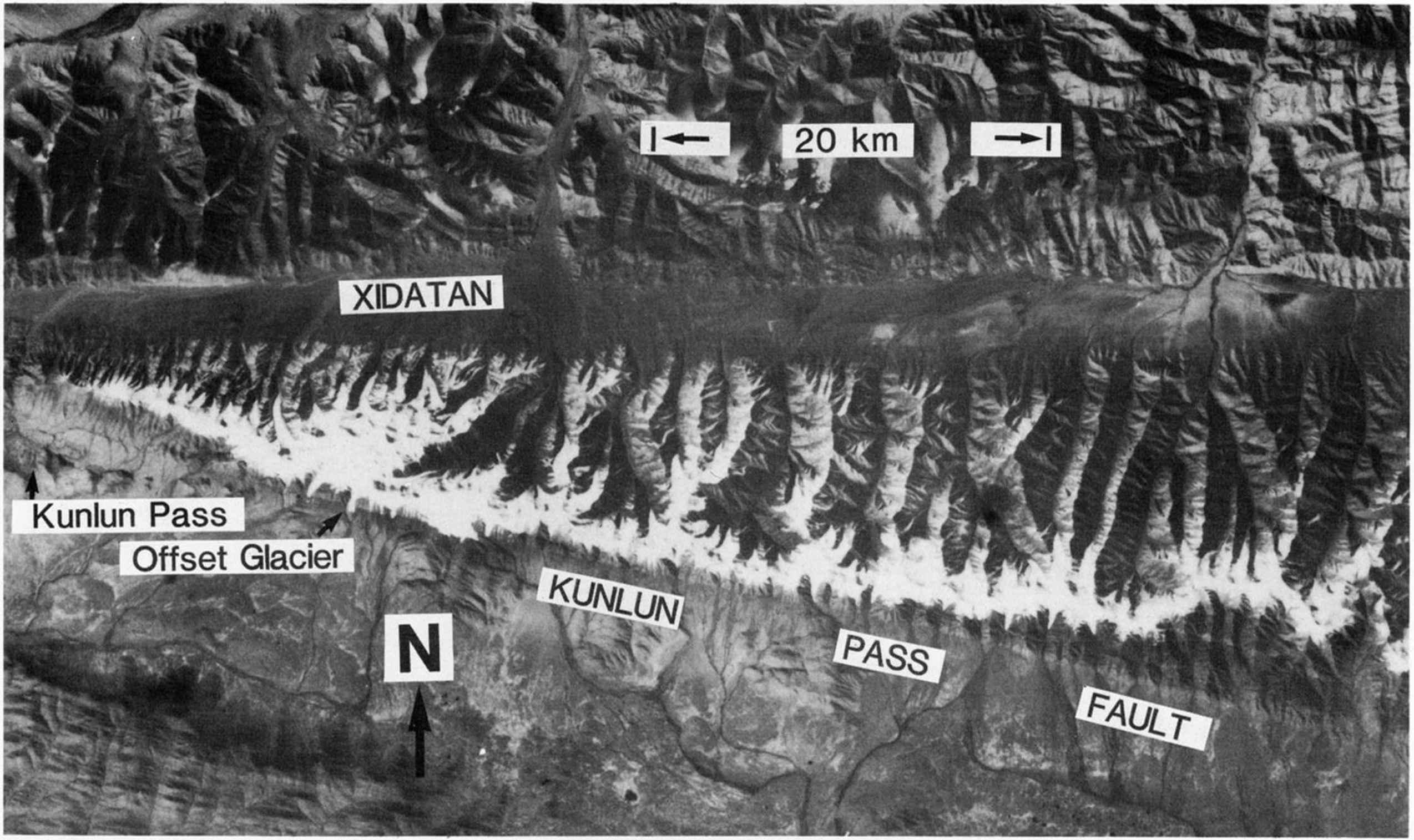

FIGURE 14. Large format camera photograph of the Kunlun Pass fault, showing the clear topographic expression of the fault and the location of the offset glacier (figure 18).

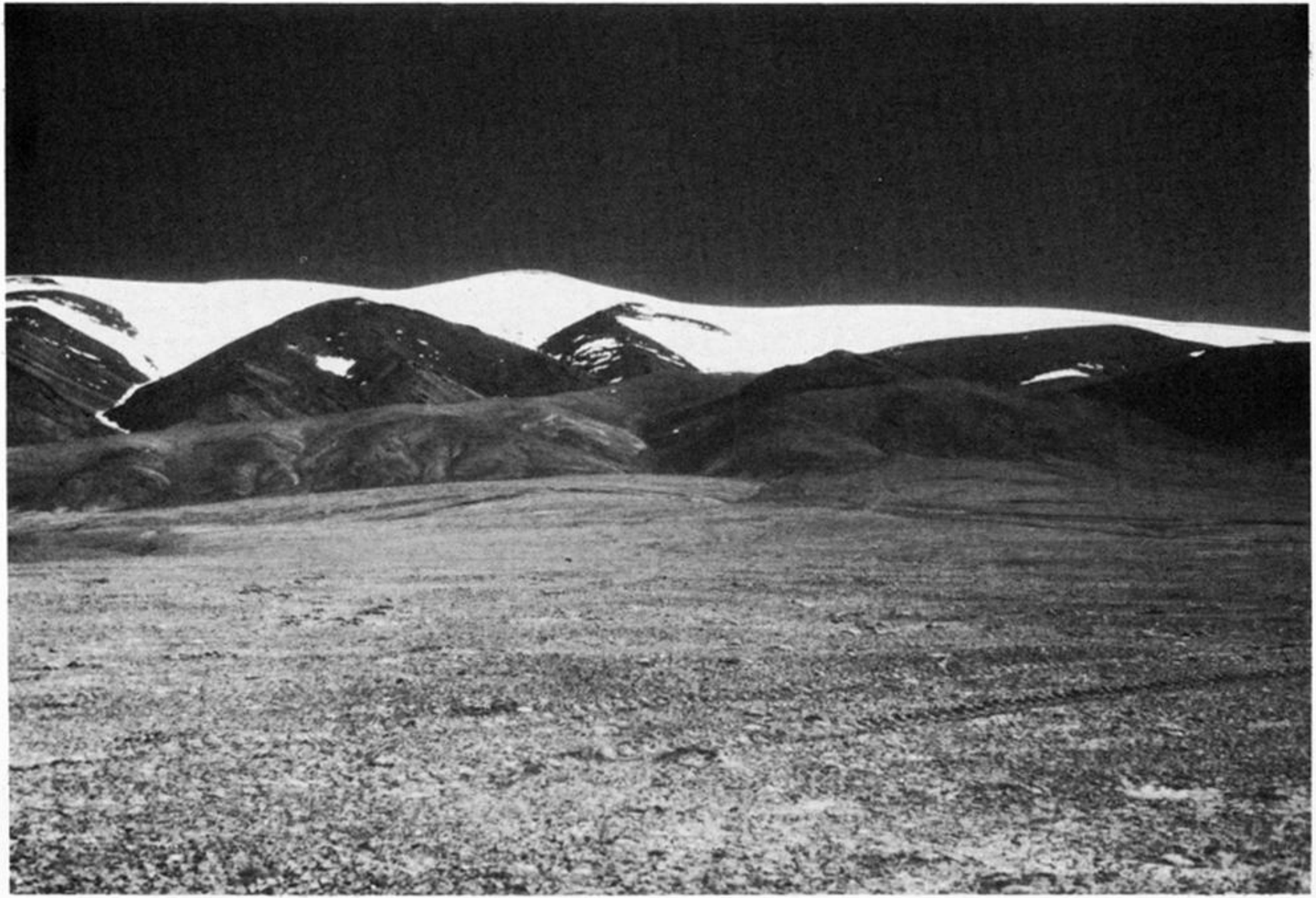

FIGURE 15. Photo looking north at an offset stream along the Kunlun Pass fault. The stream in the valley in the centre of the photo flows toward the photographer, but at the foot of the nearer hills it is displaced to the right (east) 49 ± 4 m.

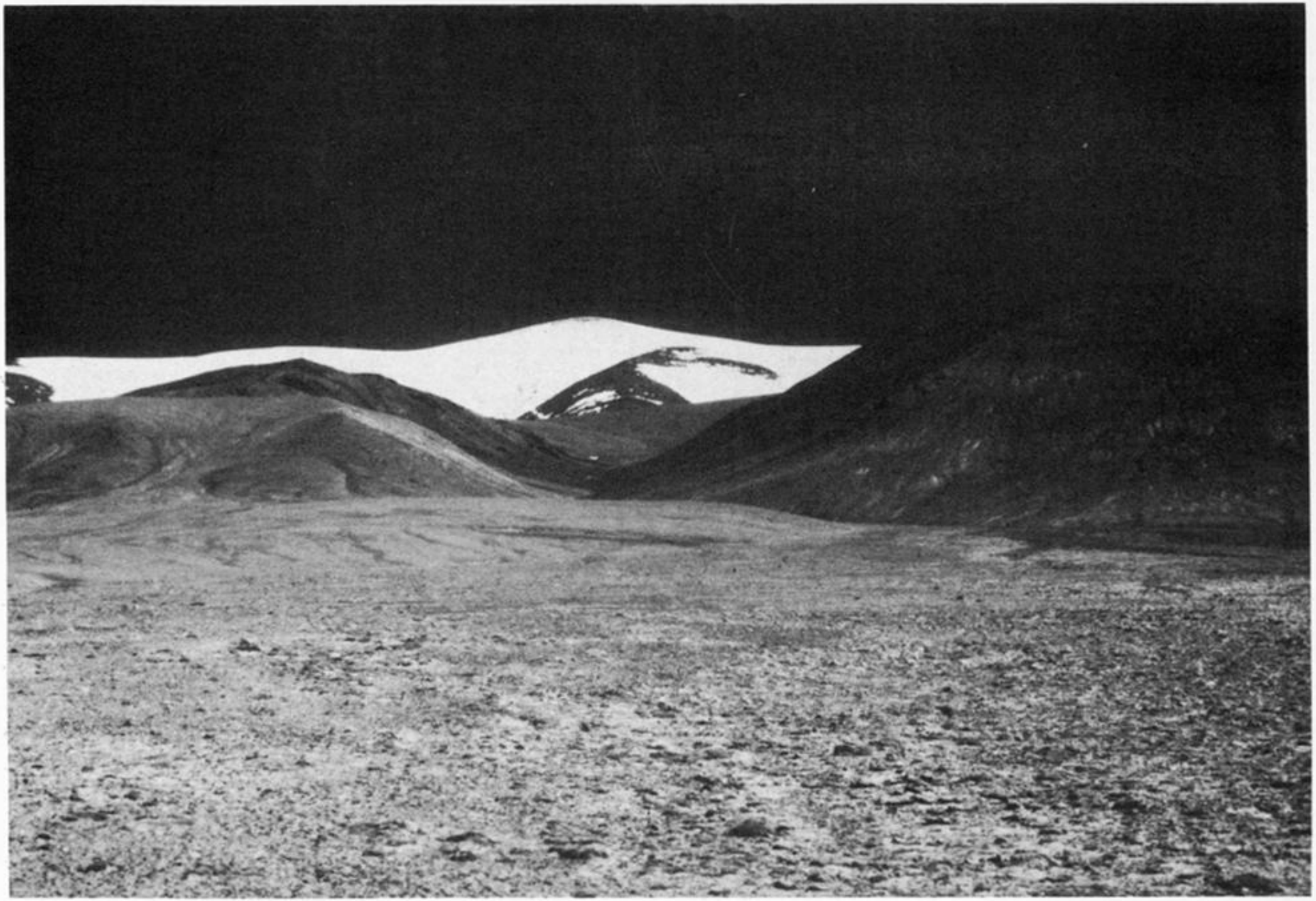

FIGURE 16. Photo looking north at a second offset stream along the Kunlun Pass fault. The valley in the centre of the photo is the same one shown on the right edge of the photo in figure 15. Again the stream flows directly toward the photographer but is offset at the Kunlun Pass fault, at the foot of the hills. The amount of offset is 95 ± 6 m.

FIGURE 18. Photo looking north at a major glacier flowing south from the highest peak in the Burhan Budai. Where the glacier reaches the Kunlun Pass fault at the foot of the mountains, it is offset about 70 m (see also figure 14). The terminal moraine of the receding glacier is offset between 100 and 150 m. Since this moraine probably was left by the last glaciation some 10 ka to 18 ka, the average rate of slip during Holocene time probably has been about 10 mm/a.

FIGURE 19. Photo looking west along the Xidatan–Tuosuohu–Maqu fault in its western segment near D in figure 13. The dark linear zone in the middle foreground is a tension gash obliquely crossing a shutter ridge that recedes from the photographer. Sag ponds farther in the distance have formed by segments of shutter ridges blocking the northerly-flowing streams.

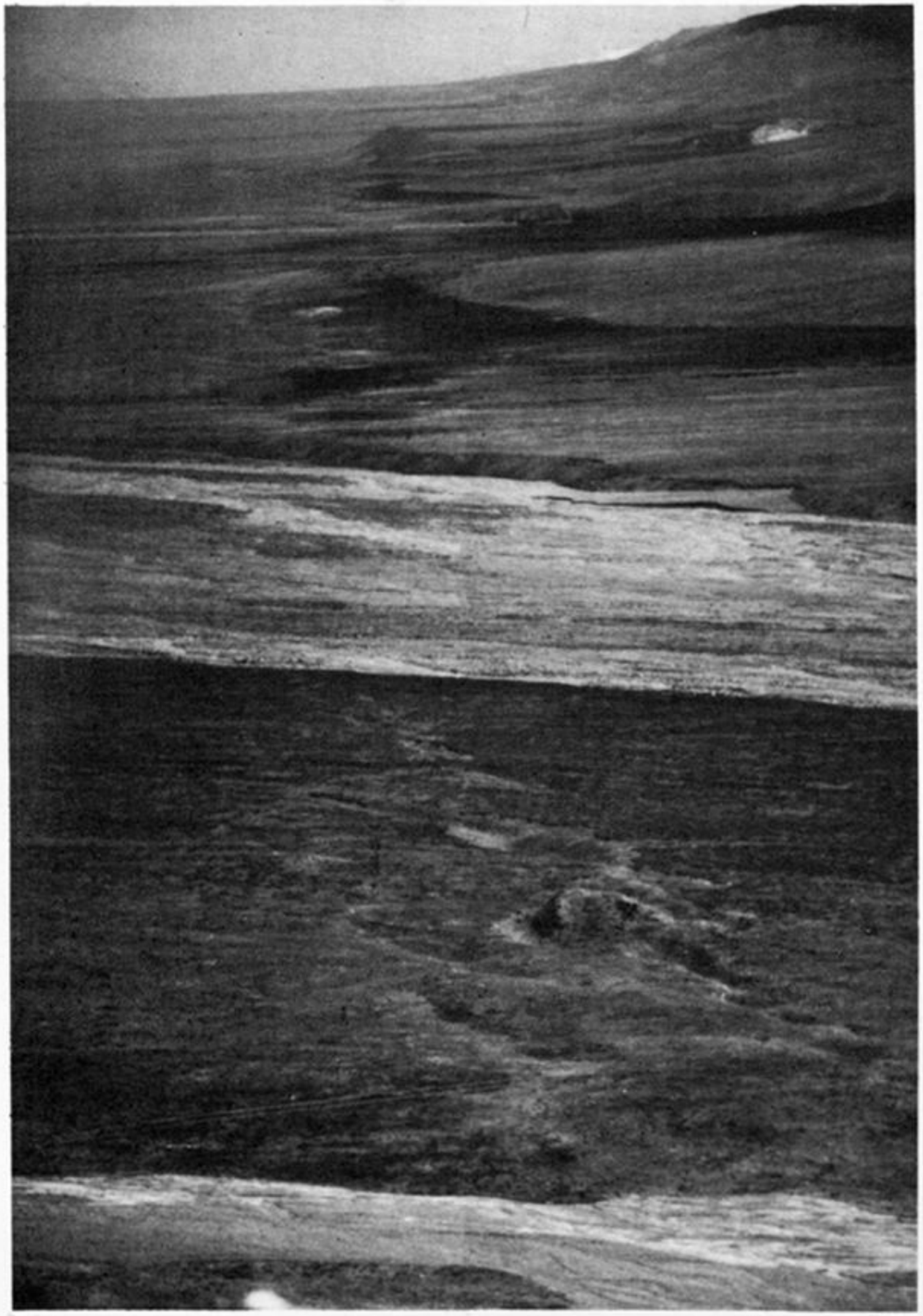

FIGURE 20. Photo (taken with a lens with a focal length of 135 mm) looking west along the Xidatan–Tuosuohu–Maqu fault from a hill near the locality I in figure 13. Streams in the foreground and the middle of the photo have obliterated evidence of surface faulting. Between the streams a small man-made hill lies within a zone of large tension gashes that trend northeast–southwest (see figure 21). In the distance, the fault has formed a ground-water barrier that is manifested by dark areas of more lush vegetation than on the neighbouring alluvial fans.

FIGURE 21. Photo taken from the man-made hill shown in figure 20 and looking east along the Xidatan–Tuosuohu–Maqu fault (J in figure 13). Doyle Watts is shown standing in a large tension gash, which trends northeast–southwest. The depth is nearly 2 m. As in figure 20, the fault is defined clearly by the darker vegetation growing on and adjacent to it in the distance.

FIGURE 24. Photo looking north-northwest at a small offset of a small stream gully. The gully entering the photo on the left trends north and is offset about 10 ± 2 m before reaching a wide braided stream. This locality is labelled V in figure 23.

FIGURE 25. Photo looking east along the Xidatan–Tuosuohu–Maqu fault and showing sag ponds and a shutter ridge in the Dongdatan (W in figure 23). Drainage from the south (right) is blocked by the shutter ridge that recedes from the left lower edge of the photo across and away to the middle of the photo. A dry sag pond in the middle of the photo is about 20 m wide. The height of the shutter ridge is as much as 5 m higher than the dry bottom of the sag pond.

FIGURE 26. Photo looking southwest toward a huge tension gash within a high shutter ridge in the Dongdatan (W in figure 23). Michael Ward, standing in the tension gash, stands about 180 cm tall.

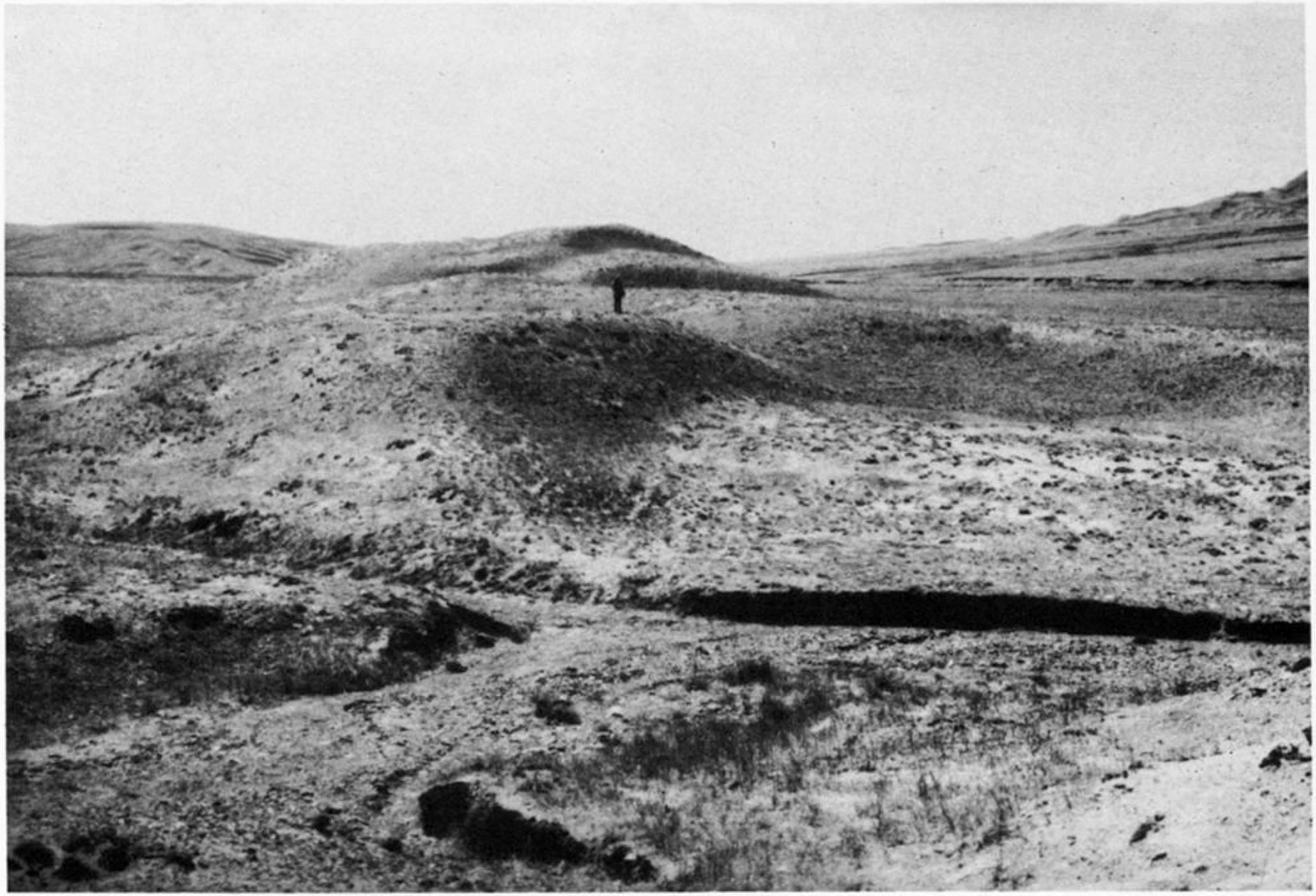

FIGURE 27. Photo looking west along the shutter ridge and the escarpment where the contour map in figure 28 was made. Two north-flowing streams join in the foreground where they cross the fault. Bill Kidd stands just south of (to the left of) a large area in which stream cobbles are exposed in groups. These cobbles apparently were deposited by the stream in the foreground when the flat area once lay closer to the photographer.

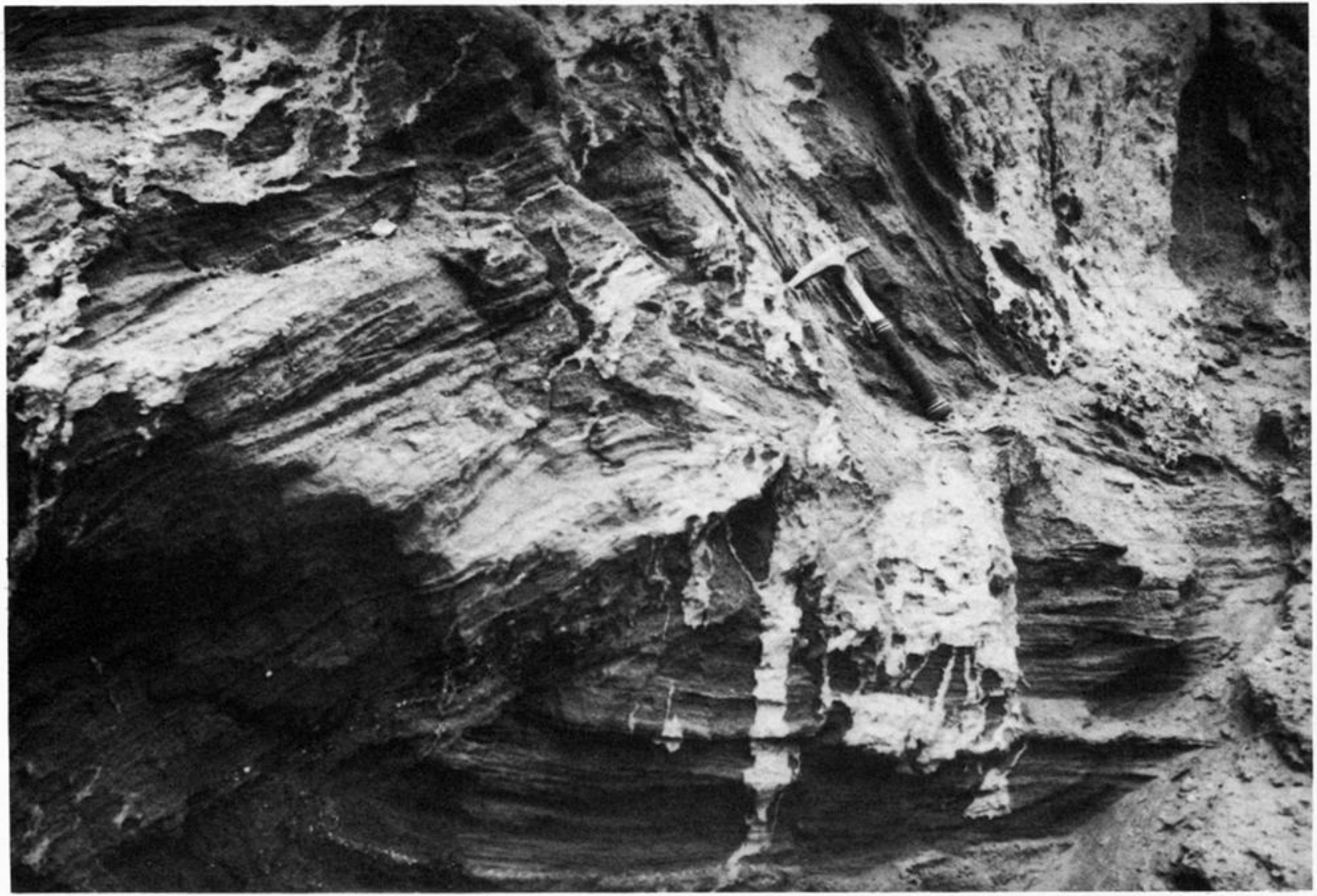

FIGURE 29. Photo, looking east, of a small thrust fault in sand and gravel deposited within the fault zone in the Dongdatan (Y in figure 23) and deformed by the formation of a shutter ridge.

FIGURE 30. Photo, looking east, of a small fold in stream gravels within a shutter ridge in the Dongdatan (Y in figure 23). The hammer in the centre of the photo gives a scale; the gravel is folded into an overturned fold with a steep northern flank. Left of the hammer the gravel beds dip nearly vertically, but to the right they are nearly flat. The overlying sand reveals the same folding but less clearly than the gravel.

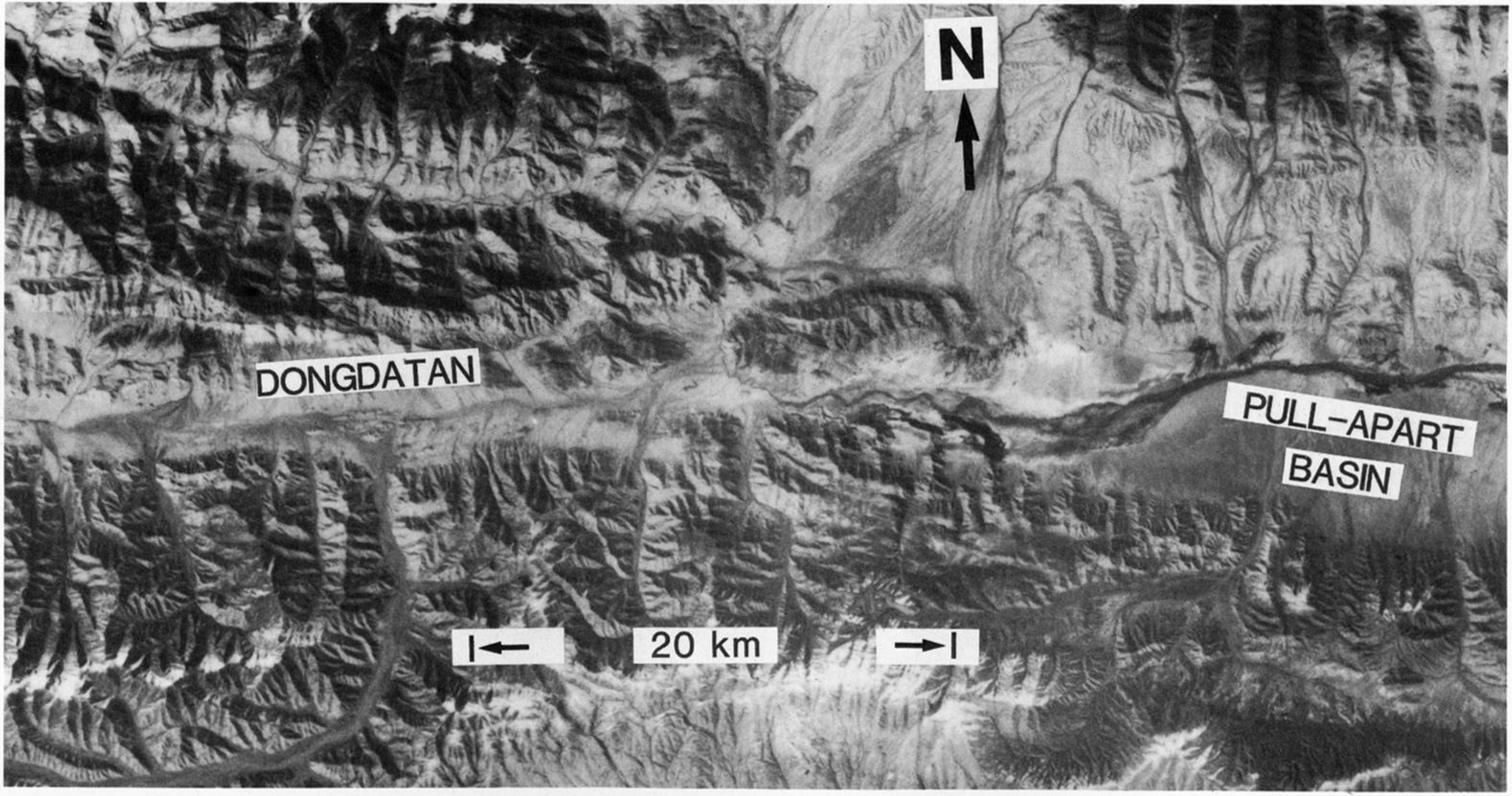

FIGURE 31. Large format camera photograph of the Dongdatan and the pull-apart basin to the east. Although the recent trace lies within the valley, segments of it have a clear topographic expression.